St. John's University

St. John's Scholar

2021

THE ION CHANNEL TRPM7 REGULATES ZINC DEPLETION-INDUCED MDMX DEGRADATION

Herui Wang
Saint John's University, Jamaica New York

Recommended Citation

THE ION CHANNEL TRPM7 REGULATES ZINC DEPLETION-INDUCED MDMX
DEGRADATION

A dissertation submitted in partial fulfillment

of the requirements for the degree of

DOCTOR OF PHILOSOPHY

to the faculty of the

DEPARTMENT OF BIOLOGICAL SCIENCES

of

ST. JOHN'S COLLEGE OF LIBERAL ARTS AND SCIENCES

at

ST. JOHN'S UNIVERSITY
New York
by
Herui Wang

Date Submitted   3/19/2021   Date Approved   03/26/2021

_____   _____

Herui Wang   Dr. Yan Zhu

ABSTRACT

THE ION CHANNEL TRPM7 REGULATES ZINC DEPLETION-INDUCED MDMX
DEGRADATION

Herui Wang

Zinc deficiency has been linked to human diseases including cancer. p53, a zinc-containing transcription factor, is the most frequently mutated tumor suppressor protein in human cancer. MDM2 and MDMX are zinc- containing proteins and crucial negative regulators of p53, which have been found to be amplified or overexpressed in various cancers. To investigate the effects of zinc depletion on the p53 signaling pathway, we have used ion chelators TPEN and bispicen as well as zinc-deficient medium to treat cells. We report here that zinc depletion results in MDMX degradation in a ubiquitination-independent and 20S proteasome-dependent manner. Restoration of zinc recovers the cellular levels of MDMX. Further, TPEN treatment inhibits growth of the MCF-7 cells, a breast cancer cell line that remains wild type p53, which is partially rescued by over-expression of MDMX. Moreover, we identified TRPM7, a zinc-permeable ion channel, as a novel MDMX- interacting protein. TRPM7 stabilizes and induces ectopic MDMX migration changes on SDS-PAGE. Depletion of TRPM7 attenuates while TRPM7 overexpression facilitates the recovery of MDMX upon adding back zinc to TPEN-treated cells. Importantly, we found that TRPM7 inhibition, like TPEN treatment, decreases breast

cancer cell MCF-7 proliferation and migration. The inhibitory effect on cell migration upon TRPM7 inhibition is also partially rescued by over-expression of MDMX. Together, our data indicate that TRPM7 regulates cellular levels of MDMX in part by modulating the intracellular $Zn2+$ concentration to promote tumorigenesis.

ACKNOWLEDGEMENTS

First, I would like to thank my mentor, Dr. Yan Zhu, for all the guidance, advice, and patience during my PhD project. Your knowledge and insightful ideas sharpen my thinking and optimize my work.

I would also like to thank my committee members: Dr. Yu, Dr. Ruggiu, Dr. Vancurova, and Dr. Yangnot only for being my committee members, but also support of my study. Additionally, I appreciate my friends Dr. Wang and Dr. Li for technical support and encouragement. Finally, I need to express gratitude to our former and current lab members Jamie Contreras, Harman Chopra, Zara Khan, Abanob Sedrak, Asha Thuraisamy, Vinh Nguyen, Olivia Hu, Ryan Pangilinan, Kulsum Asha, AlessandroProvvido, Sally Lien and Alishba Khan for all the assistance and understanding.

TABLE OF CONTENTS

LIST OF FIGURES

Abbreviations

ATM   Ataxia telangiectasia mutated

ATR   Ataxia telangiectasia and Rad3 related

Chk1   Checkpoint kinase 1

Chk2   Checkpoint kinase 2

GAPDH   Glyceraldehyde 3-phosphate dehydrogenase

H2AX   H2A histone family member X

IDPs   Intrinsically disordered proteins

TRPM7   Transient receptor potential cation channel, subfamily M, member 7

TPEN   N,N,N',N'-tetrakis(2-pyridinylmethyl)-1,2-ethanediamine

MDM2   Murine double minute 2

MDMX   Murine double minute X

Rb   Retinoblastoma protein

Rpn1   26S proteasome non-ATPase regulatory subunit 2, also as known as 26S
               Proteasome Regulatory Subunit Rpn1

Rpn2   26S proteasome non-ATPase regulatory subunit 1, also as known as 26S
               Proteasome Regulatory Subunit Rpn2

Rpn11   26S proteasome non-ATPase regulatory subunit 14, also known as 26S
               proteasome non-ATPase subunit Rpn11

Chapter I. General Introduction

Zinc is indispensable to living organisms

Zinc is the second most abundant transition metal in living organisms (Vasak & Hasler, 2000). It plays a crucial role in many biochemical processes through both structural and catalytic functions. It has also been shown to have a direct regulatory role in cellular signalingpathways (Mocchegiani, Muzzioli, & Giacconi, 2000). Through zinc coordination proteins properly fold peptide chains, stabilize structure and catalyze substrates. Cysteines and histidines in proteins are usually found to coordinate with zinc ions to form zinc fingers, a small structural motif. Zinc fingers are widely found in DNA transcription factors, RNA polymerase, assembly of proteins, hormone receptors, and apoptosis regulators. Zinc deficiency is linkedto a variety of human diseases including cancers such as bladder, breast, esophageal, head and neck, prostate, and skin cancer (Franklin & Costello, 2007).

Genome guardian p53

p53, a tumor suppressor protein encoded by TP53 gene locating on chromosome 17 in human, got this name because of its molecular mass: 53 kDa band on SDS-PAGE. Normal cells have low level of p53 proteins with short half-life. Under normal condition, the functions of p53 proteins are strictly inhibited and p53 proteins are degraded through ubiquitin- proteasome pathway (Haupt, Maya, Kazaz, & Oren, 1997; Kubbutat, Jones, & Vousden, 1997).In response to various cellular stresses including DNA damage, p53 proteins are modified to avoid inhibition and degradation, and

obtain extended half-life (C G Maki & Howley, 1997; Maltzman & Czyzyk, 1984). Stabilized and activated p53 proteins mediate cellular outcomes including induction of cell cycle arrest, apoptosis, cellular senescence, DNA repair, and inhibition of angiogenesis and metastasis through both transcription-dependent and independent mechanisms (Meek, 2015; Vousden & Prives, 2009).

p53 structure

p53 proteins (Figure I.1) have two transcription-activation domains at N-terminal (residues 1-67): activation domain 1 (TAD1, residues 1-42) and activation domain 2 (TAD2, residues 55-75). Fusion of either domain with GST could bind TATA binding proteins in vitro, and fusion with Gal4 proteins activates reporters to different level in vivo (Candau et al., 1997;Chang, Kim, Lee, Choi, & Sung, 1995). Proline rich domain (PR, residues 64-92) contains five PXXP copies that are required for p53-mediated promotion of apoptosis and repression of cellgrowth. Deletion of proline rich domain fails to induce PIG3 and loses ability to produce reactive oxygen species (ROS) (Venot et al., 1998). This domain is also necessary for the growtharrest induced by Gas 1 (Ruaro et al., 1997). Central DNA-binding domain (residues 102-292)directly binds to DNA, which requires zinc corporation. Mutations at zinc binding site, such as R175H, make p53 misfold and abolish p53's DNA binding ability, therefore prevent transcription of target genes. Nuclear localization signal (NLS) domain (residues 300-323) mediates the translocation of p53 from cytoplasm into nucleus. Critical amino acids are needed for nuclear importation. Mutations on Lys-305 and Arg-306 cause less migration of p53 into nucleus (S.-H. Liang & Clarke, 1999; S. H. Liang, Hong, &

Clarke, 1998). Oligomerization domain (OD, residues 326-356) oligomerize p53 intro

tetramer and is necessary for p53 binding to DNA. Mutations in this region reduce

p53's transcriptional activity (Kawaguchi et al., 2005). The nuclear export signal

domain (NES) locating in tetramerization domain (residues 340-351) is highly

conserved leucine-rich domain and mediates export of p53 from nucleus through

association with CRM1 (Stommel et al., 1999). C-terminal regulatory domain (CTD)

(residues 356-393) nonspecifically bind to DNA and enhances p53 transcriptional

activity.
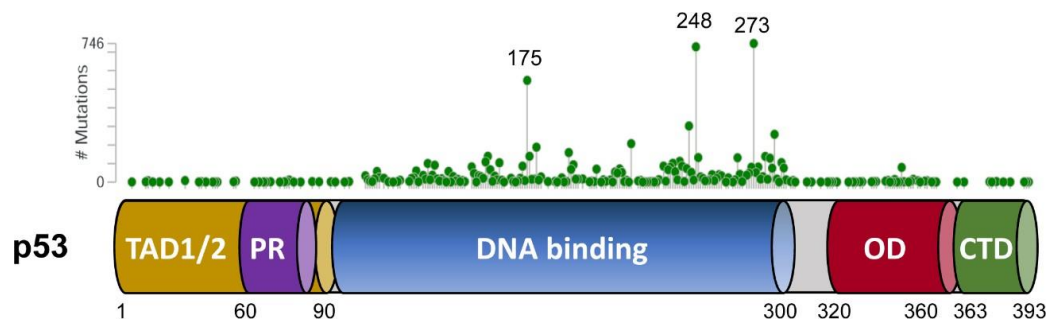
Figure I. 1. Schematic of p53 protein structure. p53 contains an N-terminal transactivation domain (TAD), which can be further divided into subdomains TAD1 and TAD2, followed by a proline-rich region (PRR). The DNA-binding domain and the oligomerization domain (OD) are connected through a flexible linker region. The regulatory C-terminal domain (CTD) is located at the extreme carboxyl terminus of the protein. The vertical line with dots indicates the number of missense-mutations in human cancer for each residue. The analysis was carried out using cBioPortal. The most frequently mutated residues R175, R248, and R273 were marked. (Zhu et al., 2018)

p53's roles in arrest of cell cycle

The progress of cell cycle is under the control of cyclin-dependent kinases (Cdks)

and their regulator cyclins. Cdks have no kinase activity unless they form complex

with cyclins. DNA damage arrests cell cycle at two checkpoints: G1/S transition and

G2/M transition. In response to genotoxic stress as well as other stress signals, active

p53 mediates cell cycle arrest through transcriptional activation of proteins that

repress cyclins and Cdks, giving cell times for DNA repair. Through binding to the promoter of p21 gene (a CDK inhibitor), p53 proteins activate transcription of p21 mRNA. p21 proteins bind to cyclin E-Cdk2 and cyclin D-Cdk4 complexes and inhibit the phosphorylation of Retinoblastoma (Rb) induced by Cdk2 andCdk4 (Harper, Adami, Wei, Keyomarsi, & Elledge, 1993). The phosphorylation status of Rb decides whether cells enter S phase or stay at G1 phase. Hypophosphorylated Rb binds and inhibits E2F transcriptional factors that activate DNA replication and genes required for S phase. Cdk2 and Cdk4 phosphorylate Rb so that cell cycle continues. Through inactivating Cdk2 and Cdk4, p21 keeps Rb dephosphorylated and blocks cell cycle progression. In additionto arrest G1/S, p53 also mediates arrest of cell cycle at G2/M transition though induction of p21 and 14-3-3σ. 14-3-3σ sequesters cyclin-B1-cdc2 complexes that trigger cell division in cytoplasm (Chan, Hermeking, Lengauer, Kinzler, & Vogelstein, 1999; Hermeking et al., 1997).p21 colocalizes with cyclin A and cyclin B1 in nucleus, associated with inactive cyclin-Cdk complexes (Dulić, Stein, Far, & Reed, 1998). In addition to activate genes that hold cell cycle,p53 can directly bind to promoters of genes that repress cell cycle. For instance, repression ofcdc25C by p53 arrest cell cycle at G2/M status (St Clair et al., 2004).

p53's roles in programmed cell death

In response to stimuli such as DNA damage, oncogene activation and oxidative stress, active p53 proteins mediate programmed cell death through both transcription-dependent and independent mechanisms.

Nuclear p53 activates transcription of pro-apoptotic genes such as Noxa or Puma

while represses transcription of anti-apoptotic genes such as Bcl2 and Survivin. Additionally, cytosolic pool of p53 translocates to outer membrane of mitochondria, where p53 inhibits anti-apoptotic factor Bcl2 and promotes oligomerization of Bax and Bak through DNA binding domain (Pietsch et al., 2008), resulting in pore formation and subsequent release of apoptoticfactors. The released apoptotic factors, such as cytochrome c, activate caspases to cleave cellular components and finally induce apoptosis. Cleavage of full-length PARP (116kDa) into89kDa and 24kDa fragments by caspases is an early indicator of apoptosis. The caspase-3 is proteolytically activated by caspase-9, which can be blocked by mutant p53 binding to procaspase-3 (Frank, Pietsch, Dumont, Tao, & Murphy, 2011).

The translocation and activation of p53 are results of post-translational modifications. Inunstressed cells, cytosolic p53 is inactivated and polyubiquitinated by MDM2 and then degraded in 26S proteasome. Upon DNA damage, p53 is phosphorylated at Ser46 by HIPK2, which triggers incorporation of Pin1 and a phosphorylation-dependent conformation change. This conformational change switches MDM2 from polyubiquitinating to multi- monoubiquitinating p53, which is a sign of nuclear export and mitochondrial translocation. The phosphorylated p53 on Ser46 after DNA damage also induces expression of proapoptoticgene p53-regulated Apoptosis-Inducing Protein 1 (p53AIP1) (Oda et al., 2000). p53 can also be fused to mitochondrial import leader peptide ornithine transcarbamylase at N-terminal, which targets p53 for mitochondrial translocation and reduces p53's transactivation ability (Mihara et al., 2003). After arrival at mitochondria, p53 is deubiquitinated by

HAUSP and bindsto Bcl2 and Bcl-xL proteins through DNA binding domain. Interaction with MDMX facilitates p53 binding to Bcl2 (Mancini et al., 2009).

Role of p53 in cancer

p53 is a major suppressor of cancer development. Lost of p53 functions is critical to cancer formation. Mutant p53 is founded in about 50% of human cancer. The Li-Fraumeni Syndrome patients who have germ line p53 mutations are more likely to get cancer. It has been shown that viruses, such as SV40 and HPV, can inhibit p53 and lead to cancer (Vogelstein, Lane, & Levine,2000).

In human cancers that remain wild-type p53, p53's functions are impaired, which weaken signaling pathways that p53 participates in. TP53 gene mutations are very common in human cancers and they often produce deficient p53 proteins (Hollstein, Sidransky, Vogelstein, & Harris, 1991; Soussi & Beroud, 2001; Vogelstein et al., 2000). In most of cases, mutant p53 proteins result from missense mutations that substitute amino acids. DNA binding domain is favored by mutations, despite mutations can distribute throughout TP53 gene. The 'hotspot' mutation sites in DNA binding domain concentrate on residues R175, G245, R248, R249, R273, and R282 (Figure I.1). Mutant p53 proteins can form tetramer with wild-type p53 to inactivate tumor suppressor functions, when mutant and wild-type TP53 gene coexist (Milner & Medcalf, 1991). In addition to inactivate wild-type p53, mutant p53 may obtain oncogenic ability through gain-of-function (GOF) mechanism. Their GOF are proved by introduction of mutant p53 into p53-null cells. Mutant p53 can promote tumorigenesis by increasing resistance to apoptosis, elevating migration and invasion

of cancer cells, and disrupting genome stability.

Although TP53 gene mutations are frequent to see, not all tumors bear TP53 mutations and their oncogenesis grow in pathways that impair wild-type p53. p53 is activated by upstream regulators through modifications in response to stress signals. Mutations or reduced expression of upstream regulators, such as ATM and Chk2, were found to reduce p53activation. The mutations on p53's downstream genes also reduce the inhibitory effect of p53.For instance, mutant p21 or 14-3-3σ fails to suppress cell cycle. In addition, overexpression ofp53 inhibitors, including MDM2 and MDMX, leads to abnormal cell proliferation.

p53 inhibitor MDM2

The murine double minute 2 (MDM2) protein, a major p53 protein inhibitor, was clonedand identified in transformed mouse cell line 3T3-DM. The human homologue of this proteinis also called as HDM2. MDM2's oncogenic potential was discovered as its overexpression induces tumorigenicity (Fakharzadeh, Trusko, & George, 1991). Amplifications of MDM2 gene in human cancers are not rare cases, especially in soft tissue sarcomas and brain tumors (Oliner, Kinzler, Meltzer, George, & Vogelstein, 1992).

MDM2 structure

MDM2 protein has 491 amino acids and contains three important domains (Figure I.2): an N-terminal domain, a central domain including an acidic domain and a C-4 zinc finger region,and a C-terminal Ring domain. The hydrophobic region (residues

1-100) in N-terminal domain (residues 1-126) enables MDM2 to interact with the transactivation domain of p53 and inhibit p53's transactivation ability (Kussie et al., 1996). The center acidic domain (AD) (residues 220- 300) and C-4 zinc finger domain (residues 290-335) have binding sites for many proteins that regulate MDM2's functions. Multiple ribosomal proteins (L5, L11, L23, L26, L27, S3, S7, S14, S15, S20, S25, S26, and S27) bind to MDM2 through this region to inhibit MDM2 and activate p53 in response to ribosomal stress (Deisenroth et al. 2016). Binding of ARF to AD promotes degradation of MDM2 and stabilizes p53 (Sherr, 2006; Y. Zhang, Xiong, & Yarbrough, 1998). Binding of p300, a transcriptional coactivator of p53, to AD attenuates p300-mediated p53 acetylation and thus inhibits DNA binding and transcriptional activity of p53 (Grossman et al.,1998; Kobet, Zeng, Zhu, Keller, & Lu, 2000). The C-4 zinc finger domain is a RanBP2 type zinc finger. Several cancer-associated mutations in this region disrupt MDM2-mediated p53 ubiquitination and degradation and (Dai & Lu, 2004; Lindström, Jin, Deisenroth, White Wolf, & Zhang, 2007; Y. Zhang et al., 2003). The Ring domain at C-terminal (residues 430-480) contains Cis3-His2-Cis3 consensus that coordinates two zinc ions (Lai, Freedman, Levine, & McLendon, 1998). Corporation of zinc folds Ring domain properly and confers MDM2-MDMXinteraction. The Ring domain of MDM2 has E3 ubiquitin ligase activity (Fang, Jensen, Ludwig,Vousden, & Weissman, 2000). In steady cells, Ring domain of MDM2 ubiquitinates p53 at lysine residues and target p53 for proteasome-dependent degradation. This ubiquitination is interfered by post-translational modification on p53 and MDM2 so that p53 avoids degradation and gets activation

(Fang et al., 2000).
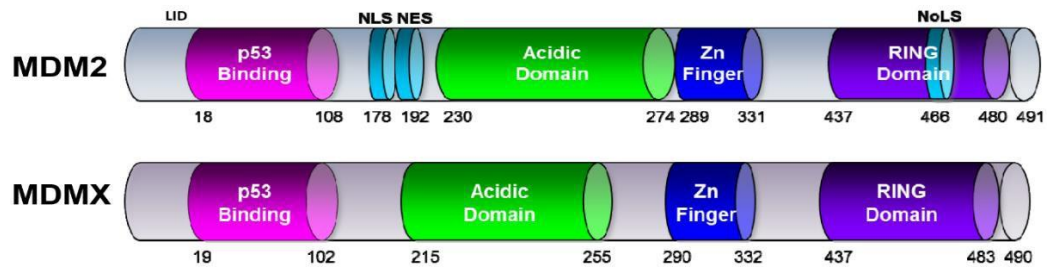
Figure I. 2. Domain structure of MDM2 and MDMX. MDM2 and MDMX each contains an N-terminal p53- binding domain, a center acidic region and zinc-finger domain, as well as a C-terminal RING finger domain. MDM2 also contains nuclear localization signal, nuclear export signal, and nucleolar localization signal sequences, which are not existed in MDMX. MDM2 and MDMX share 54% and 53% identity in their p53-binding and RING finger domain (Zhu et al., 2018).

MDM2 regulating p53

MDM2 is a downstream gene of p53 and serves as negative regulator of p53. MDM2 canrepress p53 at both ubiquitination dependent and independent manners. In human cancers with wild-type p53, amplification of MDM2 gene results in elevated MDM2 protein level andsuppression of p53 (Momand, Jung, Wilczynski, & Niland, 1998; Oliner et al., 1992).

MDM2 mediated ubiquitination-independent repression of p53

The hydrophobic region within MDM2's N-terminal interacts with N-terminal of p53 andinhibits p53's transactivation ability (Kussie et al., 1996). Gly58, Glu68, Val75, and Cys77 in MDM2 are essential for p53 binding (Freedman, Epstein, Roth, & Levine, 1997). Phe19, Trp23,and Leu26 in p53 are the most important residues for MDM2 degradation (Böttger et al., 1997; J. Chen, Marechal, & Levine, 1993). A truncated MDM2, containing only N-terminal 130 aminoacids, is able to reduce p53-mediated transactivation (Leng, Brown, Shivakumar, Deb, & Deb,1995). MDM2 also interferes

acetylation or promotes deacetylation of p53 to obstruct transactivation of p53 (Dingding Shi & Gu, 2012). CBP or its structural homology p300 bind to N-terminal of p53, and acetylate lysine at C-terminal of p53 and thus stimulate p53 transcriptional activity, while this interaction is blocked by MDM2 through binding to the N- terminal region of CBP/p300 (Gu & Roeder, 1997; Wadgaonkar & Collins, 1999). Through recruiting HDAC1, a histone deacetylase, MDM2 deacetylates p53 and reduces activity of p53, resulting in unstablizition of p53. This process can be reversed by mutant HDAC1 (Ito et al., 2002).

MDM2 mediated ubiquitination-dependent repression of p53

Ubiquitin is a small protein with molecular weight 8.6 kDa. Proteins conjugated with ubiquitin are usually marked for proteasome-dependent degradation. Conjugation of ubiquitin requires three types of enzymes: ubiquitin-activating enzymes (E1s), ubiquitin- conjugating enzymes (E2s), and ubiquitin ligases (E3s). E3s specifically transfer ubiquitin to target proteins (Pickart, 2001). An addition type of enzyme, E4 ubiquitin ligases (E4s), enhances elongation of ubiquitin chains induced by E3s on substrates (Koegl et al., 1999). MDM2's Ring domain serves as an E3 ligase that mediates monoubiquitination and polyubiuitination of p53 in a ratio-dependent manner. High amount of MDM2 mediates polyubiquitination of p53 and nuclear degradation. In contrast, low amount of MDM2 induces monoubiquitination of p53 and nuclear export (M. Li et al., 2003). CBP and p300 function as E4s to catalyze polyubiquitination of p53 driven by MDM2 (Grossman et al., 2003; D. Shi et al.,2009). E3 ligase of MDM2 is controlled by phosphorylation. c-Abl induced phosphorylation on

Y394, an amino acid close to Ring domain, reduces interaction between MDM2 and p53 to protect p53 from degradation (Goldberg et al., 2002; Sionov et al., 2001). ATM-induced phosphorylation on S395 weakens nuclear export of p53 and slows down p53 degradation after DNA damage (Khosravi et al., 1999; Maya et al., 2001). Coordination of zinc ions are necessary for E3 ligase ability of MDM2's Ring domain. Removal of zinc by TPEN treatment and mutations of zinc-binding amino acids abrogate p53 ubiquitination (Fang et al., 2000).

MDM2 facilitates substrates' interaction with proteasome subunits

Proteins can be degraded by proteasomes in ubiquitin-dependent or ubiquitin-independent way. Presence of 19S particles is not essential, but a 20S core of proteasome is necessary for a ubiquitin-independent degradation. MDM2 contributes to both pathways, because MDM2 does not only ubiquitinate substrates, but also promotes association of substrates to proteasomes. MDM2 associates with subunits within 19S proteasome regulatory particles, including S2, S4a, S5a, S6a, and S6b, and facilitates the association of p53 with the proteasome (Kulikov et al., 2010). The 20S core are made up of two layers of alpha and beta subunits. In addition to 19S regulatory subunits, MDM2 is able to mediate retinoblastoma protein (Rb) and p21 degradation in a ubiquitin-independent manner by facilitating the interaction of Rb or p21 with 20S alpha subunit 7 (Patima Sdek et al., 2005; Touitou et al., 2001).

p53 inhibitor MDMX

MDMX (murine double minute X, also known as MDM4), a homologous protein of MDM2,got this name because of its structural similarity to MDM2. Mouse MDMX was

identified earlier than human MDMX. The binding of MDMX to p53 was detected in vitro and in vivo (Shvarts et al., 1997; Shvarts et al., 1996). MDMX gene is constitutively expressed, evidencedby stable mRNA level, unlike increased MDM2 gene expression in response to stress signals (Jackson & Berberich, 1999). MDMX serves as a key negative regulator of p53 that is necessary for embryogenesis. MDMX-null mice displayed an embryonic lethality due to the loss of p53 inhibition and they were rescued by lose of TP53 gene (Parant et al., 2001). Aberrant expression of MDMX occurs in many tumors. One important difference between MDMX and MDM2 is that the Ring domain of MDMX, unlike MDM2, does not have E3 ligase ability. Therefore, MDMX cannot mediate p53 ubiquitination alone. However, MDMX can bind to MDM2 through their Ring domain. This Ring interaction enhances the efficiency of ubiquitinating p53. In contrast to MDM2, MDMX has neither nuclear import sequence nor nuclear export sequence. The absence of localization signal makes MDMX primarily localize incytoplasm. The shuttle of MDMX into nucleus needs association with partners, like MDM2.

MDMX functional regions

Human MDMX protein (Figure I.2) is made up of 490 amino acids containing a conserved p53-binding domain at N-terminal, an acidic domain and a zinc finger region in the middle, and a conserved Ring domain at C-terminal. MDMX has an observed mass around 80kDa, more than the predicted 54kDa because of post-translational modification. The residues 23-109 at N-terminal of MDMX form a complex with the residues 17-28 of p53, the transactivation domain (Popowicz,

Czarna, & Holak, 2008). Phosphorylation of residues at N-terminal affects binding of

MDMX to p53. Phosphorylation of Y99 sterically block MDMX binding to p53, while

phosphorylation of Y55 enhances binding. The central domain (residues 150-350)

includes an acidic domain and a RanBP2 type zinc finger region. The acidic domain

interacts with DNA binding domain of p53 and inhibits DNA binding activity of p53,

which requires CK1α phosphorylating S289 of MDMX (L. Chen, Li, Pan, & Chen, 2005;

Wei et al., 2016). The RanBP2 type zinc finger (residues 292-340) region suppresses

chromosome loss and multipolar mitosis in p53-deficient cells (Matijasevic,

Krzywicka-Racka, Sluder, Gallant, &Jones, 2016). The Ring domain of MDMX (residues

421-490) does not have E3 ubiquitin ligaseactivity, unlike MDM2, but is able to stabilize

MDM2 from ubiquitin degradation and stimulate MDM2's E3 activity through

formation of MDM2-MDMX heterodimer via their Ring domains, contributing to

better efficiency of inhibition and ubiquitin-dependent degradation of p53 (Linares,

Hengstermann, Ciechanover, Müller, & Scheffner, 2003; Sharp, Kratowicz, Sank, &

George, 1999; Tanimura et al., 1999). The Ring domain of MDMX has a conserved

C2H2C4 motif that coordinates two zinc ions and maintains Ring domain's functions.

An intact Ring domain serves as binding sites for regulatory proteins. For example,

ARF binds to both full- length MDMX and truncated MDMX. However, in order to

translocate MDMX into nucleus tosequester them, the Ring domain has to be present

(Jackson, Lindstrom, & Berberich, 2001).Single amino acids within Ring domain also

play important roles to the functions of MDMX. Substitution of cysteine 463 to alanine

of human MDMX compromises MDM2 interaction andreduces p53 inhibition, though

N-terminal of MDMX retains ability to bind to p53. Mdmx C462A/C462A (a mouse mutation equivalent to human MDMX C463A) mice died at embryonicdevelopment stage due to uncontrolled p53 activation, indicating Ring domain of MDMX is necessary for p53 inhibition (Huang et al., 2011).

MDMX stability in response to stress is under control of post-translational modifications

In response to stress signals, inhibition of p53 by MDMX is rapidly relieved through degradation of MDMX, while MDM2 is involved in this process through mediating MDMX ubiquitination and targeting MDMX for ubiquitin-dependent proteasome degradation. Switch MDM2's target from p53 to MDMX needs post-translational modifications on protein p53, MDM2 and MDMX relating to phosphorylation, acetylation, ubiquitination et al.

MDMX modifications follow DNA damage

Ionizing radiation – induced DNA damage activates ATM (Ataxia telangiectasia mutated)to directly phosphorylate MDMX on S403 (Y. Pereg et al., 2005). As a primary signal transducer of DNA damage, ATM also activates Chk2(Checkpoint kinase 2) which in turn phosphorylatesMDMX on S342 and S367 (L. Chen, Gilkes, Pan, Lane, & Chen, 2005). Phosphorylation on theseserine residues, especially S367, enhances 14-3-3 binding to MDMX, leading to translocationof MDMX into nucleus (LeBron, Chen, Gilkes, & Chen, 2006; Yaron Pereg et al., 2006). MDMXprotein level is maintained by interaction with deubiquitinase HAUSP (herpes virus-associated ubiquitin specific protease 7) under normal condition, but this interaction is decreased upon ATM-

dependent phosphorylation after DNA damage, contributing to MDMX degradation (Meulmeester et al., 2005). MDMX degradation following DNA damage is mediated by MDM2in ubiquitin-dependent proteasome pathway, which requires phosphorylation of MDMX. Evidence shows that mutation serine367 to alanine impairs binding of 14-3-3 to MDMX and reduces MDM2-mediated ubiquitination and degradation (Kawai et al., 2003; Okamoto et al.,2005).

Following UV-C treatment, MDMX is phosphorylated at S367 by Chk1, instead of Chk2, which then enhances binding of 14-3-3γ to MDMX and reduces p53 ubiquitination (Yetao Jinet al., 2006).

DNA damage induced by genotoxic drug Doxorubicin stimulates ATM-activated c-Abl (Abelson non-receptor tyrosine kinase) to phosphorylate MDMX on Y99 and Y55, while phosphorylated Y99 impairs interaction with p53, but not Y55. This process is independent of S342, S367 and S403 phosphorylation (Zuckerman et al., 2009).

MDMX is involved in responses to hypoxia

Hypoxia activates p53 in an ATR-Chk1 cascade, during which Chk1 phosphorylates MDMXat S367, stimulating 14-3-3γ binding to MDMX. Among S342, S367 and S403, S367 is the most critical amino acid for 14-3-3γ binding as mutation of S367 completely abolishes binding. In contrast to S367, mutation of S342 remains little 14-3-3γ binding and S403 mutation does notimpair interaction (Lee et al., 2012).

MDMX regulation in response to ribosomal stress

Ribosomal stress leads to activation of p53, requiring proteasome-dependent MDMX degradation mediated by MDM2. Ribosomal stress induced by Actinomycin

or low dose of 5-FU does not stimulate phosphorylation of MDMX on S367 and 14-3-3 binding, indicating mechanisms of regulating MDMX different from DNA damage. Ribosomal proteins L5, L11 andL23 bind to acidic domain of MDM2 and inhibits p53 ubiquitination, in which L11, but not L5 and L23 stimulates MDMX degradation (Gilkes, Chen, & Chen, 2006). Ribosomal subunit S7 stabilizes p53 through MDM2 inhibition in a MDMX-dependent way (Zhu et al., 2009). In contrast, ubiquitination of MDMX by MDM2 is interrupted by non-coding 5S rRNA under non-stress conditions, through binding to Ring domain of MDMX (M. Li & Gu, 2011).

Proteasome-mediated protein degradation

Proteins are degraded in cells through two major ways: lysosome degradation and proteasome degradation. Turnover of proteins, such as transcription factors, regulates cellular activities, and prevents accumulation of damaged proteins. Proteasome-mediated ubiquitin degradation pathway has been well studies. In this pathway, proteins are first labeled with polypeptide ubiquitin, and then degraded by 26S proteasome. However, it has been proven that proteasomes not only proteolyze ubiquitin-tagged proteins. Proteins can be degraded byproteasome independent of ubiquitination. In this case, unstructured region within proteins is the signal of this ubiquitin-independent degradation. It is difficult to distinguish ubiquitin- dependent and ubiquitin-independent degradation because some proteins can be degraded through both pathways. Furthermore, most proteasome inhibitors block both 20S and 26S proteasome as they are targeting 20S core, which is shared by 26S proteasome.

Ubiquitin-dependent proteasome pathway

Ubiquitin is a polypeptide consisting of 76 amino acids (8.6KDa). Addition of one ubiquitin molecule to one lysine residue of protein is monoubiquitination. Monoubiquitination can occur on multiple residues of proteins and affects localization of proteins. In many cases, monoubiquitination marks nuclear exportation of proteins and lysosomal degradation. Monoubiquitination is the prerequisite for polyubiquitination because ubiquitin chains are elongated on the first ubiquitin molecule (Komander, 2009). Polyubiquitinated proteins can be degraded by 26S proteasome in cytoplasm and nucleus.

Ubiquitination requires multiple steps. Ubiquitin-activating enzyme (E1), ubiquitin- conjugating enzyme (E2) and ubiquitin ligase enzyme (E3) are involved in a basic ubiquitination. Ubiquitin is first activated by E1 through formation thioester bond between E1and ubiquitin in an ATP-dependent way. Secondly, the activated ubiquitin is transferred fromE1 to cysteine of E2 and forms thioester bond again, which is an ATP-dependent process too. E3 recruits ubiquitin-conjugated E2 and specifically transfer ubiquitin from E2 to a lysine residue of protein substrate. The ubiquitin and lysine interact to each other through isopeptide bond (Hershko & Ciechanover, 1998; Scheffner, Nuber, & Huibregtse, 1995). An additional ubiquitin ligase (E4) enhances E3-mediated ubiquitin transfer and results in polyubiquitination (Koegl et al., 1999).

The polyubiquitinated proteins are degraded by 26S proteasomes. A 26S proteasome consists of a 20S core and a 19S regulatory particle. Ubiquitin-tagged proteins are usually recognized by 19S particle, where ubiquitin chains are removed

by deubiquitinases. Subunitswithin a 19S particle drive translocation and unfolding of proteins through consuming ATP. Finally, unfolded proteins are degraded in the 20S core.

Ubiquitin-independent proteasome pathway

20S proteasomes can recognize unfolded proteins and degrade them in the absence of 19S particles, which does not require ubiquitination. Conformational changes induced by stresses lead to exposure of hydrophobic region being recognized. 20S proteasome-mediateddegradation is promoted in response to oxidation (Giulivi, Pacifici, & Davies, 1994; Kisselev, Kaganovich, & Goldberg, 2002). In addition to proteins affected by stresses, native proteins with large unstructured region that are considered as intrinsically disorder proteins (IDPs) are also degraded by 20S proteasomes.

The 20S proteasome consists of 28 subunits that are categorized into alpha type and betatype. All these subunits form four layers of rings. α-type subunits constitute the two outer rings that determine what proteins will be proteolyzed. β-type subunits form the two inner rings that catalyze degradation. β1, β2 and β5 subunits possess caspase-like, trypsin-like and chemotrypsin-like proteolytic ability (Groll et al., 1999).

Proteolytic ability of 20S proteasome is regulated by binding of activators. PA200 is a large nuclear protein (200KDa) that can bind to each end of 20S proteasome to open it (Ortegaet al., 2005). PA28 α and β subunits are cytoplasm proteins that can also bind to both ends and enhances selectivity and peptidase ability. Both PA200 and

PA28 α, β can bind to one endof 20S and leave other end for 19S particle binding and form a regulator-20S-19S complex (Blickwedehl et al., 2008; Cascio, Call, Petre, Walz, & Goldberg, 2002). Another PA regulator PA γ stays in nucleus and upregulates 20S's capacity. All these activators increase 20S's protein degradation after oxidation (Pickering & Davies, 2012). Binding of regulatory proteins controls20S proteasome functions. Association of NQO1 and NQO2 (NADPH: quinone oxidoreductase)with 20S inhibits degradation of IDPs. NQO1 and NQO2 increase in response to stress stimuli, including oxidation or irradiation, and stabilize proteins containing IDR, like p53 (Asher, Tsvetkov, Kahana, & Shaul, 2005; Xu, Patrick, & Jaiswal, 2013). Association of substrates with20S proteasome is specific. It has been shown that MDM2 promotes p21 association with 20Ssubunit alpha 7, which is independent of ubiquitination (Y. Jin, Lee, Zeng, Dai, & Lu, 2003; Touitou et al.,2001; B. Wang et al., 2010).

TRPM7

TRPM7 is a ubiquitously expressed protein that has ion channel and protein kinase ability. TRPM7 localizes in plasma membrane and intracellular vesicles that are different fromendosome, lysosome and many other vesicles. These vesicles store zinc in normal condition and release zinc in response to oxidative stress (Sunday A. Abiria et al., 2017). TRPM7 shows preference of conducting Mg2+ and Ca2+, and has permeability to physiologically essential ions, like Zn2+, Mn2+, Co2+. Some environmentally toxic metals, including Ni2+, Cd2+, Ba2+ are also allowed for passing through (Monteilh-Zoller et al., 2003). TRPM7 consists of a N- terminal with four melastatin homology domains, six transmembrane segments (S1-S6)(residues 756-

1095) and a C-terminal containing transient receptor potential (TRP) region (residues 1109-1128), coiled-coil domain (residues 1198-1250), Serine/Threonine rich domain (residues 1380–1596), and the α-kinase domain (residues 1597–1821) (Figure I.3). The channel pore (residues 1039–1056) locates between S5 and S6. Two amino acids E1047 and E1052 are critical for permeability of divalent cations, especially E1047. E1047Q and E1052Q mutations greatly reduces permeation of divalent ions and the blocking of permeability is more dramatic on E1047Q (M. Li et al., 2007). TRPM7 kinase domain can autophosphorylate serine and threonine residues in its Ser/Thr rich domain and phosphorylate Ser and Thr on proteins, such as histone H3, annexin 1, myosin IIA (Clark et al.,2008; Dorovkov & Ryazanov, 2004; Ryazanova, Dorovkov, Ansari, & Ryazanov, 2004). TRPM7kinase domain affects its channel activity. Mg-ATP binding in kinase domain inhibits TRPM7 channel. Mutation (K1648R) that abolishes ATP binding in the kinase domain reduces inhibition of channel function (Demeuse, Penner, & Fleig, 2006). In addition to affect channeldomain, the C-terminal kinase domain of TRPM7 can be cleaved in a cell-type specific mannerand translocate to nucleus, where it can bind multiple components of chromatin remodelingcomplexes as well as several transcription factors containing zinc-binding domains. Binding to those zinc-finger containing proteins requires zinc (Krapivinsky, Krapivinsky, Manasian, & Clapham, 2014).

TRPM7 play roles in cell growth, proliferation, differentiation, survival through sensing stimuli in or out of cells, conducting cation flux, influencing transcription et al. Silencing of TRPM7 reduces cell growth. Abnormal TRPM7 expression is present in

various type ofcarcinomas and TRPM7 correlates with migration, invasion in cancer

cells. Overexpression ofTRPM7 was found in breast cancer and led to larger tumor

size (Guilbert et al., 2009). Chemicals that can modulate TRPM7 activities have

been identified and used to study mechanisms of TRPM7 in cells.
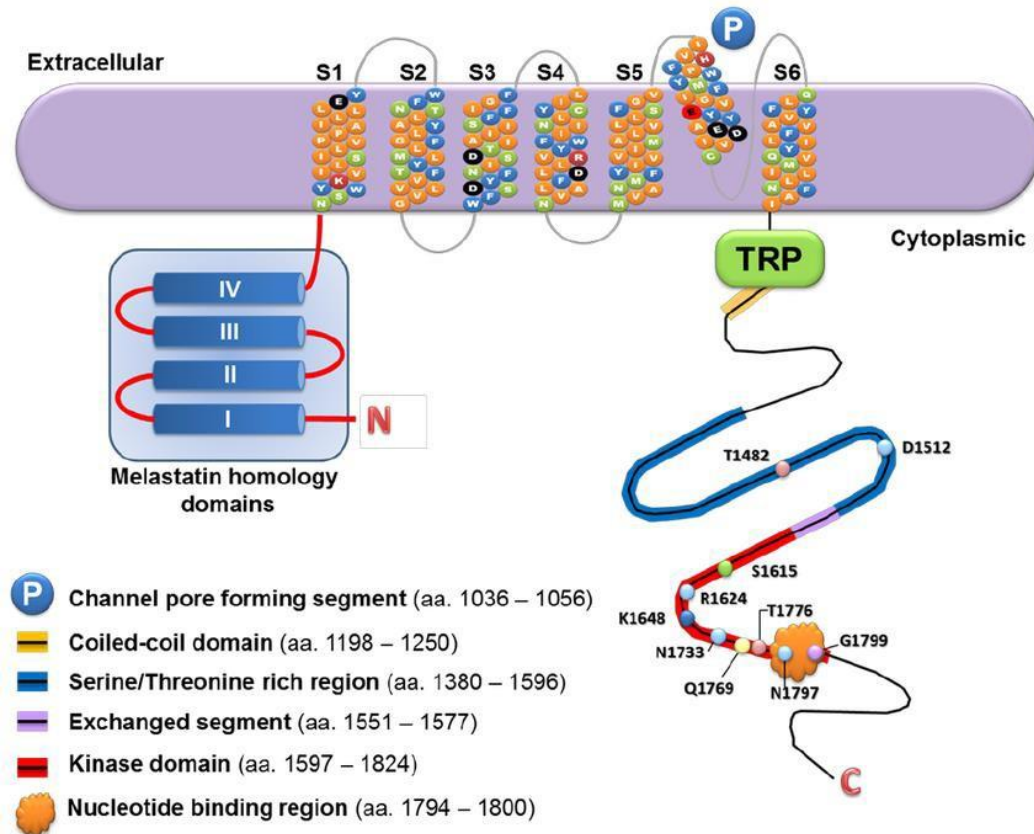
Figure I. 3. A schematic diagram to illustrate the protein structure of TRPM7 channel-kinase.
(Yee, Kazi, & Yee, 2014)

Chapter II. The ion channel TRPM7 regulates zinc depletion-induced MDMX degradation

Abstract

Zinc deficiency has been linked to human diseases including cancer. MDMX, a zinc- containing protein and crucial negative regulator of p53, has been found to be amplified or overexpressed in various cancers. We report here that zinc depletion by the ion chelator TPEN or Chelex resin results in MDMX degradation in a ubiquitination-independent and 20S proteasome-dependent manner. Restoration of zinc recovers the cellular levels of MDMX. Further, TPEN treatment inhibits growth of the MCF-7 breast cancer cell line, which is partially rescued by over-expression of MDMX. Moreover, we identified TRPM7, a zinc-permeable ion channel, as a novel MDMX-interacting protein. TRPM7 stabilizes and induces ectopic MDMX migration changes on SDS-PAGE. Depletion of TRPM7 attenuates while TRPM7 overexpression facilitates the recovery of MDMX upon adding back zinc to TPEN-treated cells. Importantly, we found that TRPM7 inhibition, like TPEN treatment, decreases breast cancer cell MCF-7 proliferation and migration. The inhibitory effect on cell migration upon TRPM7 inhibition is also partially rescued by over-expression of MDMX. Together, our data indicate that TRPM7 regulates cellular levels of MDMX in part by modulating the intracellular Zn^{2+} concentration to promote tumorigenesis.

Introduction

Zinc is the second most abundant transition metal in living organisms (Vasak & Hasler, 2000). It plays a crucial role in many biochemical processes through both structural and catalytic functions. It has also been shown to have a direct regulatory role in cellular signalingpathways (Mocchegiani et al., 2000). Zinc deficiency is linked to a variety of human cancers such as bladder, breast, esophageal, head and neck, prostate, and skin cancer (Franklin & Costello, 2007).

p53, a zinc-containing transcription factor, is the most frequently mutated tumor suppressor protein in human cancer (Vogelstein et al., 2000). The role of zinc in stabilizing wild-type p53 structure and loss of bound zinc in cancer derived mutant p53 proteins has been well documented (Y. Cho, Gorina, Jeffrey, & Pavletich, 1994; Stoner et al., 2009; Warren et al.,2013; X. Yu, Vazquez, Levine, & Carpizo, 2012). Two crucial negative regulators of p53, the homologous proteins, MDM2 and MDMX, are also zinc-containing proteins. Each has a C4 zinc-finger domain in their central region and a RING-type zinc finger domain at their C- terminus (Wade, Li, & Wahl, 2013). The C-terminal RING domain of MDM2 but not MDMX possesses an intrinsic E3 ubiquitin ligase activity and MDMX regulates MDM2 E3 ligase activitythrough RING-RING interactions (Kawai, Lopez-Pajares, Kim, Wiederschain, & Yuan, 2007). Through the RING-containing E3 ligase activity, MDM2 promotes ubiquitination and 26S proteasome-mediated degradation of both p53 and MDMX in addition to several other cellular proteins (Marine & Lozano, 2010). Zinc chelation or RING finger mutations abolish theE3 ligase activity of MDM2 (Fang et al., 2000). Moreover, it

has been reported that MDM2 facilitates p21(Y. Jin et al., 2003; Z. Zhang et al., 2004) or Rb (P. Sdek et al., 2005) degradation through its binding to the C8 alpha subunit of the 20S proteasome independent of its E3 ligase function. The central region of MDM2 contains a C4 zinc-finger domain that has been shown to interact with multiple MDM2 regulatory proteins (Fahraeus & Olivares-Illana, 2014; Manfredi, 2010). Several cancer-associated mutations have been identified in the MDM2 C4 zinc-finger domain to disrupt the MDM2-ribosomal protein interaction and attenuate MDM2-mediated p53 degradation (Lindstrom, Jin, Deisenroth, White Wolf, & Zhang, 2007). The MDMX RING domain can repress the proliferation of p53-null cells, while the zinc-finger domain of MDMX suppresses genome instability and tumor growth (Matijasevic et al., 2016).

The TRPM7 (transient receptor potential melastatin 7) is a bifunctional protein with both ion channel and α-type protein kinase feature (Runnels, Yue, & Clapham, 2001). TRPM7 is required for early embryonic development (J. Jin et al., 2008; J. Jin et al., 2012) and is abnormally overexpressed in various cancer cells (Yee, 2017). As a cation channel, TRPM7 conducts physiologically essential metal cations such as Zn^{2+}, Mg^{2+}, and Ca^{2+} as well as environmentally toxic metals such as Ni^{2+}, Cd^{2+}, and Ba^{2+} with particularly high permeation of Zn^{2+} (Monteilh-Zoller et al., 2003). The C-terminal kinase domain of TRPM7 can be cleaved and translocated to the nucleus, where it can bind multiple components of chromatin remodeling complexes as well as several transcription factors with zinc-binding domains (Desai et al., 2012; Krapivinsky et al., 2014). It has been hypothesized that TRPM7-mediated

modulation of intracellular Zn^{2+} concentration leads to epigenetic chromatin covalentmodifications that affect gene expression patterns (S. A. Abiria et al., 2017; Desai et al., 2012).Here, we report that zinc depletion results in MDMX degradation in a ubiquitination-independent and 20S proteasome-dependent manner. Adding back zinc recovers the cellular levels of MDMX while depletion of TRPM7 attenuates the effects of zinc. In addition, we show that TRPM7 interacts with and induces changed migration of the MDMX polypeptide upon denaturing polyacrylamide gel electrophoresis (SDS-PAGE) that require the TRPM7 channel function. Moreover, TRPM7 inhibition decreases MCF-7 cancer cell growth and migration, while MCF-7 cells with MDMX over-expression are more resistant to TRPM7 inhibition- mediated cell migration suppression. Together, our results indicate that TRPM7 regulates cellular levels of MDMX in part by modulating intracellular zinc concentration, which is turn may provide a new therapeutic target for combinational cancer treatment.

Results

Zinc depletion by TPEN reduces cellular levels of MDMX

In order to investigate the effects of zinc on the p53 signaling pathway, MCF-7 breast cancer cells were treated with 5 µM TPEN, an intracellular membrane-permeable zinc chelator.As shown in Figure II.1A, we found that TPEN treatment induces p53 as previously reported (Ra, Kim, Lee, & Kim, 2009). Intriguingly, the cellular levels of MDMX were dramatically reduced while the levels of MDM2 were simultaneously increased. Similarly, when we treated MCF-7 cells with bispicen,

another zinc chelator, we observed induction of p53 and MDM2 levels but reduction of MDMX levels (Figure II.1B). MDMX reduction was also observed in cells grown in zinc-deficient DMEM medium in comparison to the cells that were grown in zinc-deficient DMEM supplemented with 5 μM $ZnSO_4$, or regular DMEM medium (Figure II.1C). Note that under this condition no p53 or MDM2 induction was observed. This may be due to the fact that TPEN and bispicen are membrane-permeable agents which can deplete intracellular zinc more efficiently than the extracellular zinc-deficient medium (Y. E. Cho et al.,2007). TPEN and bispicen may also activate p53 through other mechanism(s). Nevertheless,our results demonstrate that cellular levels of MDMX are sensitive to zinc depletion. Thereduction of MDMX levels most likely happen post-transcriptionally. Quantitative-RT-PCR analysis revealed that mRNA levels of MDMX remained fairly constant during the time period of TPEN treatment (Figure II.1D). Furthermore, we found that the levels of ectopically expressed MDMX proteins in HEK293T cells also decrease upon TPEN treatment (Figure II.1E).

To show that the effects of TPEN on cellular levels of MDM2, MDMX, and p53 are due tozinc depletion but not other divalent cations, we pre-treated MCF-7 cells with 5 μM TPEN andadded back 25 μM $ZnSO_4$, $CaCl_2$, or $MgCl_2$. As shown in Figure 1F, adding back Zn^{2+} but not Ca^{2+} or Mg^{2+} reversed the effect of TPEN, as MDMX degradation was attenuated and the levelsof p53 and MDM2 were decreased and went back to the same levels as in untreated cells. Similarly, adding back Zn^{2+} also reversed the effects of bispicen on cellular levels of MDMX, MDM2, and p53 (Figure II.S1A).

The effect of TPEN was not limited to MCF-7 cells. As shown in Figure II.S1B, TPEN treatment led to reduced cellular levels of MDMX but increased levels of MDM2 and p53 in LNCaP prostate cancer cells. In PC3 cells, another p53-null prostate cancer cell line, we also observed TPEN-induced MDMX degradation. Together, our data demonstrate that zinc depletion has distinct effects on the three key components of the p53 signaling pathway. Most importantly, our results show that zinc depletion leads to MDMX degradation.
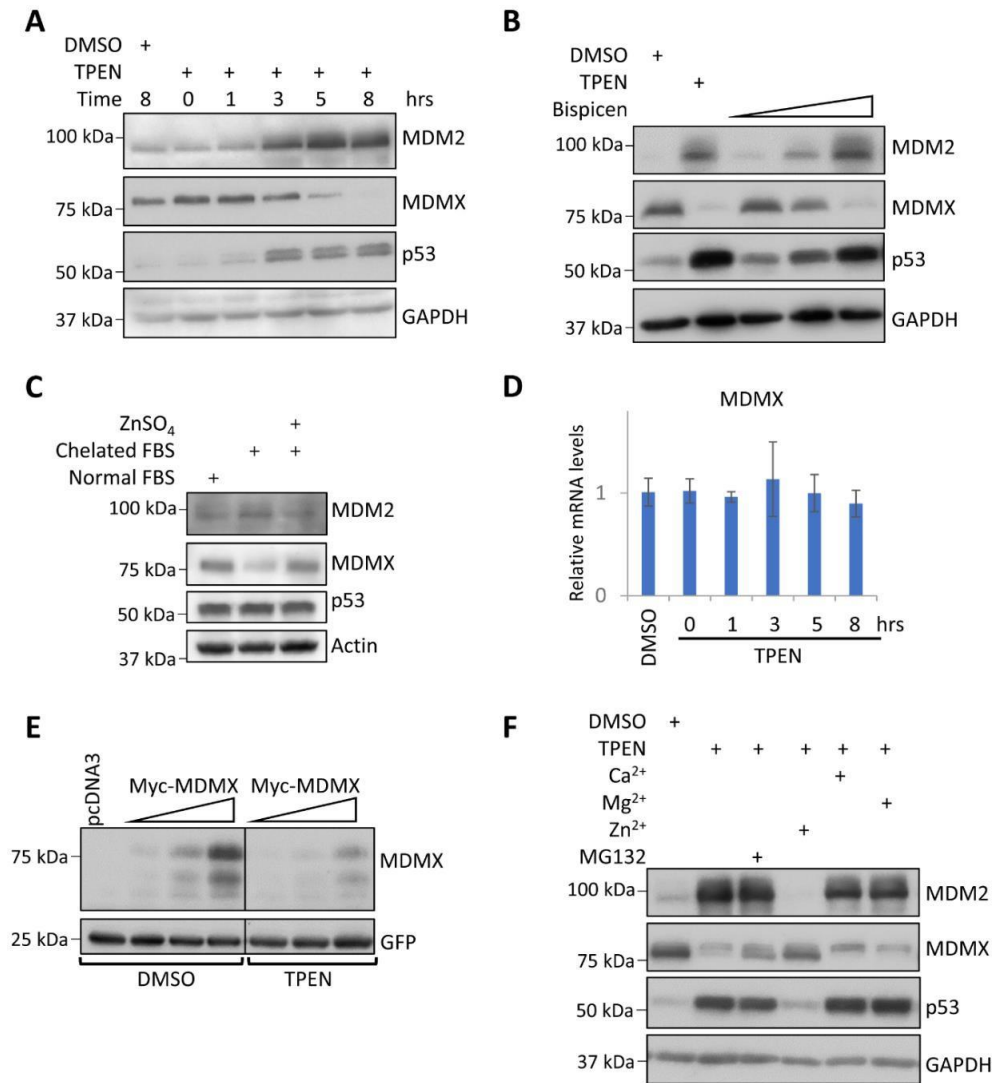
Figure II. 1. Zinc depletion represses MDMX at protein level. (A) TPEN reduces cellular levels of MDMX but increases MDM2 and p53. MCF-7 cells were treated with DMSO (control) or 5 µM TPEN and harvested at indicated time points. (B) Bispicen reduces cellular levels of MDMX. MCF-7 cells were treated with 5 µM TPEN or increasing dosages of Bispicen (10, 50, or 100 µM) for 8 hours. (C) Zinc depletion by Chelex resin reduces cellular levels of MDMX. MCF-7 cells were incubated in DMEM with 10% of normal FBS, DMEM with 10% of Chelex resin-treated FBS, or DMEM with 10% of Chelex resin-treated FBS supplemented with 5 µM $ZnSO_4$ for two days. (D) mRNA levels of MDMX remain constant after TPEN treatment. MCF-7 cells were treated and harvested as in panel A. Total RNA was extracted. Quantitative RT-PCR was carried out to check mRNA levels of MDMX. (E) TPEN reduces levels of ectopically expressed MDMX. HEK293T cells were transfected with increasing amounts of Myc-MDMX plasmids (0.15, 0.25, or 0.5 µg). GFP plasmids (0.05 µg) were also included as transfection control. Twenty-four hours after transfection, the transfected cells were treated with 5uM TPEN for 8 hours. (F) Adding back Zn2+ but not Ca2+, Mg2+ reverses the effect of TPEN on the cellular levels of MDMX, MDM2 and p53. MCF-7 cells were treated with 5 µM of TPEN for 5 hours and then 25 µM CaCl2, MgCl2, $ZnSO_4$, or MG-132 were added and incubated for 5 hours.
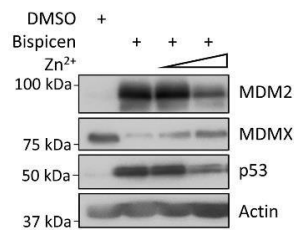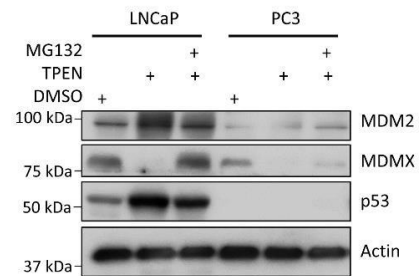
Figure II.S 1. Zinc depletion reduces cellular levels of MDMX. (A) Adding back Zn2+ reverses the effect of bispicen on cellular levels of MDMX, MDM2 and p53. MCF-7 cells were treated with 100 µM bispicen for 5 hour then 5 or 25 µM ZnSO4 were added. Five hours later, the cells were harvested and total cell lysates were analyzed by immunoblotting with indicated antibodies. (B) TPEN reduces cellular levels of MDMX in prostate cancer cells. LNCaP and PC3 cells were treated with 5 µM TPEN alone or in combination with 25 µM MG132 for 5 hours. The cells were harvested and total cell lysates were analyzed by immunoblotting with indicated antibodies.

TPEN-induced MDMX degradation is mediated by proteasome

TPEN-mediated zinc chelation can cause oxidative DNA damage and chromosome breaks (Ho, Courtemanche, & Ames, 2003) and activate cytosolic caspase activity (Hashemi, Ghavami,Eshraghi, Booy, & Los, 2007). It has been shown that proteasome-mediated degradation of MDMX occurs after DNA damage or ribosomal stress (de Polo, Vivekanandan, Little, & Yuan, 2016). In addition, it was reported that MDMX can be subjected to caspase cleavage at Glu361,leading to reduced cellular MDMX levels (Gentiletti et al., 2002). Moreover, zinc chelation may lead to MDMX misfolding for lysosomal degradation. To examine the mechanism(s) that account for TPEN-induced MDMX reduction, we pre-treated MCF-7 cells with 5 µM TPEN, and then co-treated cells with the proteasome inhibitor MG-132, or two types of lysosome inhibitor chloroquine and bafilomycin A1. We found that only MG-132 but not chloroquine or bafilomycin A1 reversed the effect of TPEN on MDMX, suggesting that TPEN-induced MDMX degradation is mediated by the proteasome but not by lysosomal-mediated turnover (Figure II.2A). Similarly, in LNCaP cells, MG-132 but not chloroquine or bafilomycin A1 co-treatment reversed the effect of TPEN on cellular levels of MDMX (Figure II.S2A). Note that both chloroquine and bafilomycin A1 inhibited LC3B-II degradation (Figure II.S2A), indicating their effectiveness under the experimental condition.

To test if caspase cleavage accounts for TPEN-mediated MDMX reduction, MCF-7 cells were treated with 5 µM TPEN in the presence or absence of the caspase inhibitor Z-VAD-FMK.We found that TPEN treatment led to reduced-levels of MDMX

regardless of the presence ofZ-VAD-FMK (Figure II.2B). Similarly, Z-VAD-FMK had no effect on TPEN-induced MDMX reduction but inhibited TPEN-induced PARP cleavage in LNCaP cells (Figure II.S2A). Additionally, we observed that TPEN treatment reduces the cellular levels of ectopically expressed wild-type MDMX as well as the mutant MDMX (D361A), a mutant that is resistant to caspase cleavage (Figure II.2C). Note that we detected a slight increase in ROS (Reactive Oxygen Species) levels in TPEN treated cells in comparison to the DMSO treated cells, but to a much lesser extent when compare to cells treated with pyocyanin, a cell-permeablecompound capable of redox cycling (Figure II.S2B). Therefore, under our experimental conditions, caspase cleavage most likely does not contribute to TPEN-induced MDMX reduction.
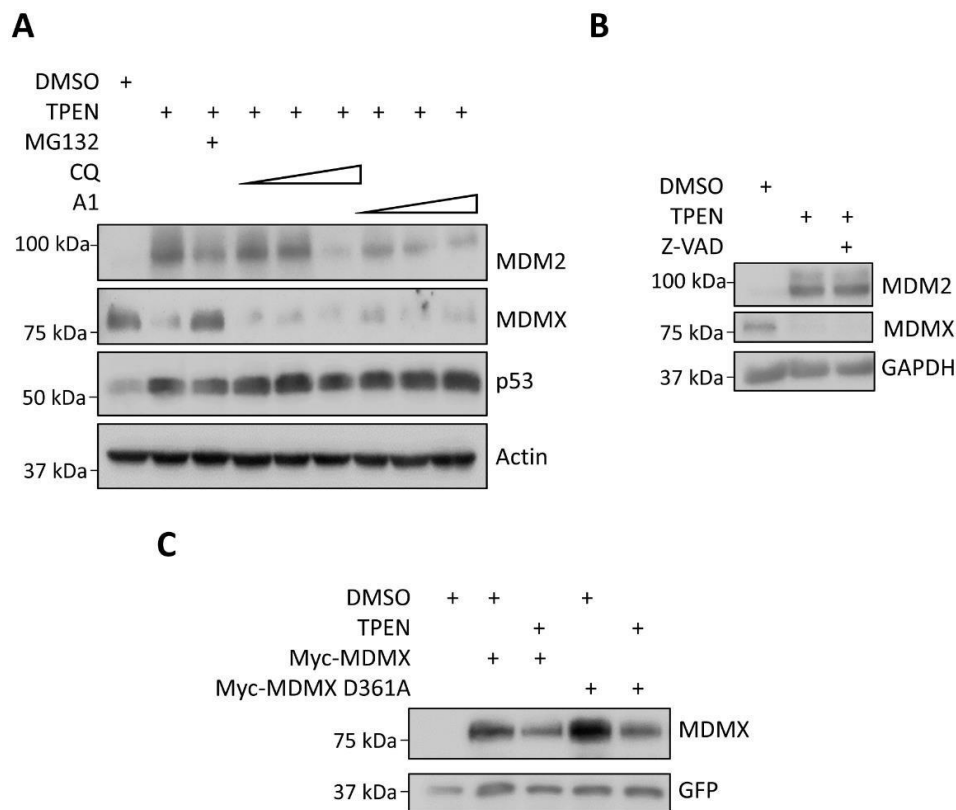
Figure II. 2. TPEN-induced MDMX degradation is mediated by proteasome but not lysosome or caspase cleavage. (A) Proteasome inhibitor MG-132 but not lysosome inhibitors protect MDMX from degradation. MCF-7 cells were treated with DMSO (control) or 5 µM TPEN for 3 hours and then MG-132 (25 µM), chloroquine (CQ: 25, 50, or 100 µM) or bafilomycin A1(A1; 50, 100, or 500 nM) were added and incubated for another 5 hours. (B) Caspase inhibitor does not prevent MDMX from TPEN-induced degradation. MCF- 7 cells were treated with 5 µM TPEN in the presence or absence of Z-VAD-FMK (25 µM) for 8 hours. (C) TPEN reduces levels of ectopically expressed MDMX caspase cleavage-resistant variant D361A. HEK293T cells were transfected with wild-type Myc-MDMX or Myc-MDMX D361A (0.15 µg). Twenty-four hours after transfection, transfected cells were treated with 5 µM TPEN for 8 hours.
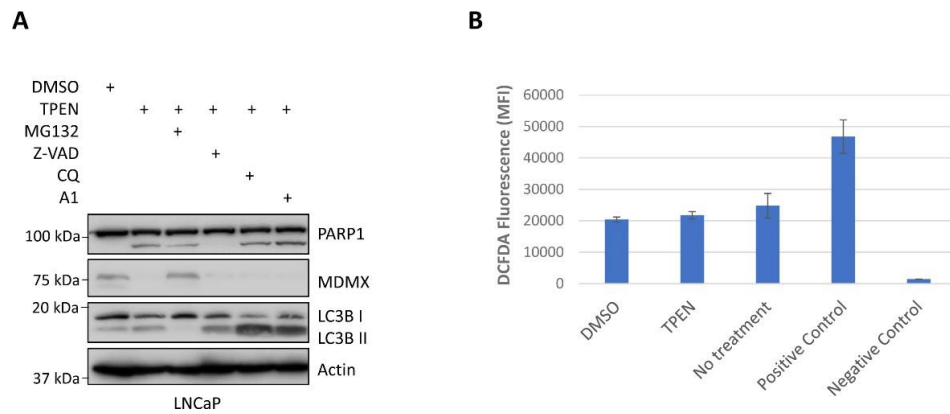
Figure II.S 2. TPEN treatment induces minimal ROS in MCF7 cells and mediates MDMX degradation through proteasome. (A) TPEN-induced MDMX degradation is mediated by proteasome. LNCaP cells were treated with DMSO or TPEN (5 µM) for 3 hours then MG-132 (25 µM), Z-VAD-FMK (25 µM), chloroquine (CQ: 50 µM) or bafilomycin A1(A1; 10 nM) were added. Five hours later, the cells were harvested and total cell lysates were analyzed by immunoblotting with indicated antibodies. (B) TPEN treatment induces minimal ROS production. 2.2 ×104 MCF7 cells per well were plated on 96-well plates in triplicates for 5 experimental groups. Eighteen hours later, two sets of triplicate cells were treated with DMSO or TPEN (5 µM) for 8 hours and cellular ROS levels were measured using ROS Detection Cell-Based Assay Kit (DCFDA). Positive control (pyocyanin treatment), negative control (N-actyl cysteine treatment), and no treatment control were also included in triplicates following the manufacture's procedure. Total DCFDA (2,7-Dichlorofluoroscin Diacetate) fluorescence was measured using an excitation wavelength at 480 nm and emission wavelength at 530 nm.

TPEN-induced MDMX degradation is mediated by 20S proteasome,independent of ubiquitination and MDM2

MDMX degradation is controlled in part by MDM2-mediated ubiquitination and proteasome degradation (Wade et al., 2013). To examine whether TPEN induces MDMX ubiquitination, we found that while MG132 treatment led to the accumulation of ubiquitinated MDMX species, no such accumulation was observed in the presence of TPEN, indicating a ubiquitin-independent mechanism (Figure II.3A). MDM2-mediated p53 ubiquitination was analyzed at the same time to confirm that the assay worked under the experimental conditions. In line with this observation, we found that two E3 ligase inhibitorsof MDM2 [HLI373 (Kitagaki, Agama, Pommier, Yang, & Weissman, 2008) and compound 1 (S.Yu et al., 2009)] cannot rescue the effect of TPEN on cellular levels of MDMX (Figure II.S3A). This is consistent with previous report showing that zinc chelation by TPEN abolishes the E3 ligase function of MDM2 (Fang et al., 2000).

As the 20S proteasome has been shown to degrade proteins that contain unstructured regions by a ubiquitin-independent mechanism (Ben-Nissan & Sharon, 2014), we speculated that zinc depletion could lead to MDMX misfolding, resulting in its 20S but not 26S proteasome -mediated degradation. To test this possibility, we co-treated MCF-7 cells with 5μM TPEN along with an increased dosage of capzimin dimer, an inhibitor of the 19S proteasome cap subunit Rpn11. The capzimin dimer did not prevent MDMX from degradation,suggesting that 26S proteasome function is not required for MDMX degradation (Figure II.3B). Furthermore, in MCF-7 cells

transfected with siRNAs targeting the 19S proteasome cap subunits PMSC2 (ATPase 2) and PSMD1 (non-ATPase regulatory subunit; a.k.a. Rpn2), TPEN induced MDMX degradation similarly as in cells transfected with control siRNA (Figure II.3C). Note that cellular levels of p53 were elevated upon inhibition of 26S proteasome function aspreviously reported (C. G. Maki, Huibregtse, & Howley, 1996). Together, our results demonstrate that in the presence of TPEN, MDMX is targeted for 20S proteasome-mediateddegradation in a ubiquitination-independent manner.

As MDM2 has been found to associate with several subunits of the 19S proteasome regulatory particle and target p53, p21 and Rb for proteasome-dependent but ubiquitination- independent degradation, we assumed that the accumulated MDM2 upon TPEN treatment would still somehow facilitate the degradation of MDMX. Accordingly, we transfected MCF-7cells with control siRNA or two different siRNAs which targets MDM2. Remarkably, TPEN induced MDMX degradation in cells treated with the MDM2 siRNAs to a similar extent as in cells treated with control siRNA (Figure II.3D). Similarly, TPEN induced MDMX degradation toa similar extent in MCF-7 cells with or without pre-treatment of MD-224, an MDM2 PROTAC degrader (Y. Li et al., 2019) (Figure II.S3B). Note that MD-224 failed to degrade MDM2 but induced cellular levels of p53 in MCF-7 cells. In 22RV1 cells, a prostate cancer cell line that MD-224 did degrade MDM2 under our experimental condition, TPEN induced MDMX degradation with or without MD-224 treatment (Figure II.S3C). Therefore, our data indicate that MDM2 is not required for TPEN-mediated MDMX degradation.
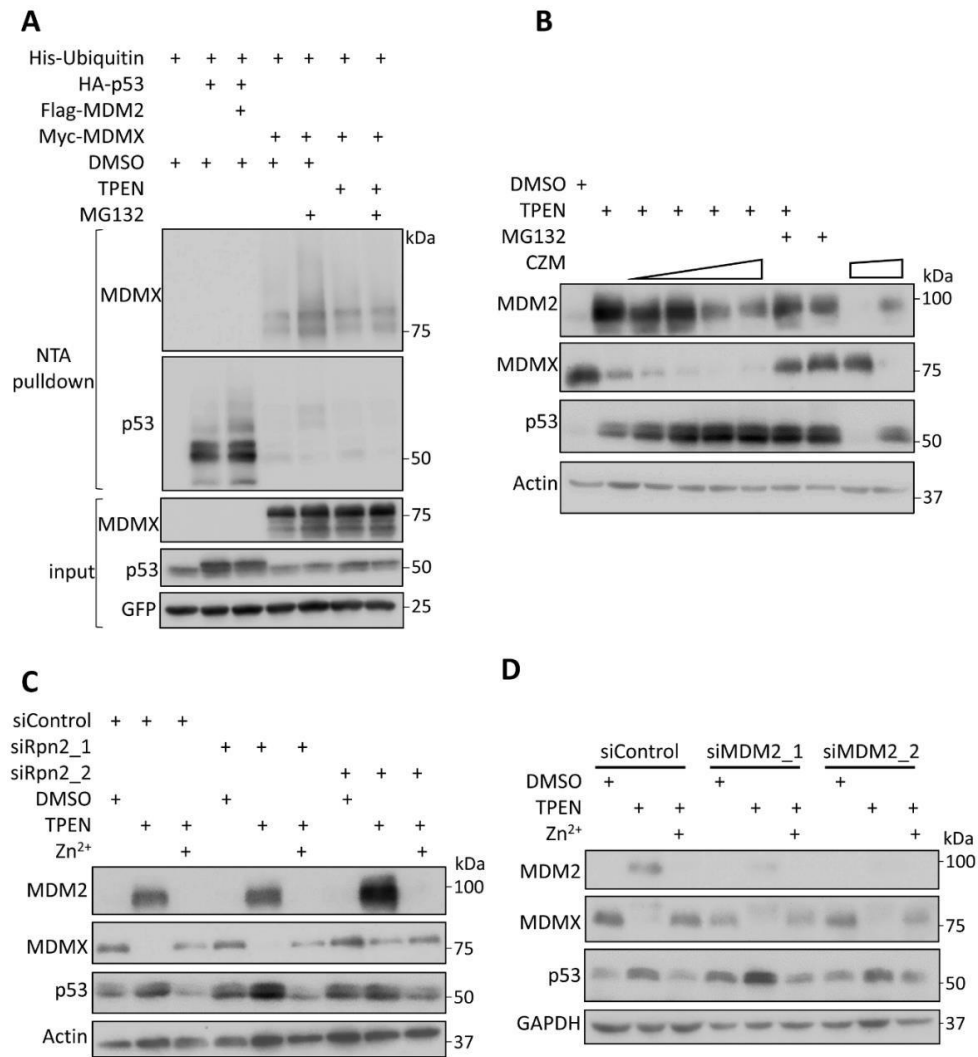
Figure II. 3. TPEN-induced MDMX degradation is mediated by 20S proteasome, independent of ubiquitination and MDM2. (A) TPEN does not induce ubiquitination of MDMX. HEK293T cells were transfected with combination of Myc-MDMX (1 µg), HA-p53 (1 µg), and His-ubiquitin (2.5 µg) plasmids as indicated. GFP plasmids (0.1 µg) were also included as transfection control. Twenty-four hours later, cells were treated with or without 5 µM TPEN for 3 hours and then 25 µM MG-132 was added and incubated for 5 hours. Total cell lysates were prepared with 1/10 of the cell lysates saved as input control. The rest were subjected to Ni-NTA-agarose beads pull-down. Both input and eluted proteins were analyzed by immunoblotting with indicated antibodies. (B) Inhibition of 19S proteasome cap subunit Rpn11 does not prevent MDMX from degradation. MCF-7 cells were treated with 5 µM TPEN in the absence or presence of capzimin dimer (2.5, 5, 10, or 20 µM), or capzimin dimer only (5 µM) for 8 hours. (C) Knock-down 19S proteasome cap subunit Rpn2 does not prevent MDMX from degradation. MCF-7 cells were transfected with siRNAs targeting Rpn2 (siRpn2_1 and siRpn2_2). Forty-eight hours after transfection, the cells were treated with 5 µM TPEN for 5 hours. Then ZnSO4 (5 µM) was added as indicated for 5 hours. (D) Depletion of MDM2 by siRNAs does not prevent TPEN-mediated MDMX degradation. MCF-7 cells were transfected with two different siRNAs targeting MDM2 (siMDM2_1 and siMDM2_2). Forty-eight hours later, the cells were incubated with 5 µM TPEN for 5 hours, and then treated with or without 5 µM ZnSO4 for another 5 hours.
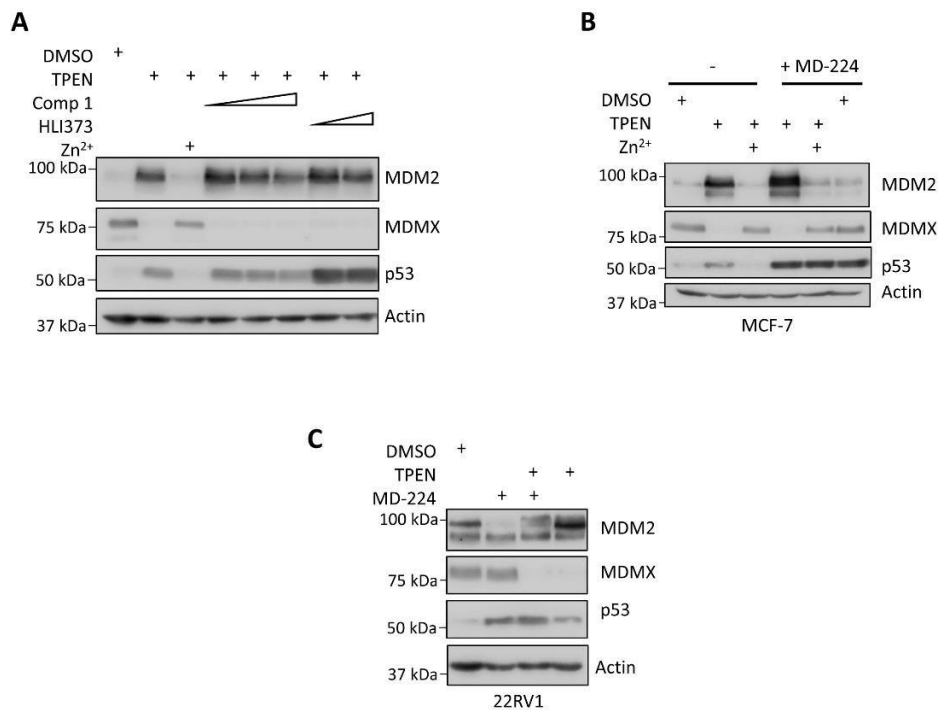
Figure II.S 3. TPEN-induced MDMX degradation is independent of MDM2. (A) MDM2 inhibitors does not protect MDMX from TPEN-induced degradation. MCF-7 cells were treated with DMSO (control) and 5 µM TPEN for 5 hours and then ZnSO4 (25 µM), compound 1 (Comp1: 6, 12, or 24 µM), or HLI373 (5 or 10 µM) was added as indicated. Five hours later, the cells were harvested and total cell lysates were analyzed by immunoblotting with indicated antibodies. (B-C) MDM2 PROTAC degrader MD-224 does not protect MDMX from TPEN-induced degradation. MCF-7 cells (B) or 22Rv1 cells (C) were pre-treated with DMSO (control) and 30 nM MD-224 for 2 hours. Both sets of cells were then treated with DMSO (control) or 5 µM TPEN for 5 hours. For MCF-7 cells, 25 µM ZnSO4 was added back in one set of TPEN treated cells as indicated. Five hours later, the cells were harvested and total cell lysates were analyzed by immunoblotting with indicated antibodies.

TPEN-induced MDMX reduction does not require MDMX phosphorylation at key serine residues

Stress-induced MDMX phosphorylation at several residues in its central domain has been shown to mediate MDMX nuclear translocation and subsequent degradation (de Polo et al., 2016). We considered that phosphorylation events are needed for TPEN-mediated MDMX degradation and transfected HEK293T cells with different MDMX variants harboring mutation at Ser347, Ser367, or Ser403. Phosphorylation on these serine residues has been shown to be critical for DNA damage-induced MDMX degradation (de Polo et al., 2016). As shown in Figure II.4A, the mutant MDMX proteins were as sensitive to TPEN treatment as wild-type MDMX. Moreover, the MDMX protein carrying mutation at all these three residues was more resistant to etoposide or doxorubicin than TPEN treatment (Figure II.4B). Furthermore, using U2OS cell clones that express mutant MDMX (S367L) from the endogenous MDMX locus, we found that endogenous MDMX S367L is more resistant to etoposide than TPEN treatment (Figure II.4C). In line with these results, TPEN treatment induced cellular levels of phosphorylated H2AX, a marker for DNA double-strand breaks, although to a much lesser extent in comparison to etoposide, a topoisomerase II inhibitor and chemotherapeutic agent (Figure II.S4). Therefore, DNA damage-induced MDMX phosphorylation may not be involved in TPEN-mediated MDMX degradation. Nevertheless, we cannot rule out that phosphorylation at other residues contributes to MDMX degradation upon zinc depletion.
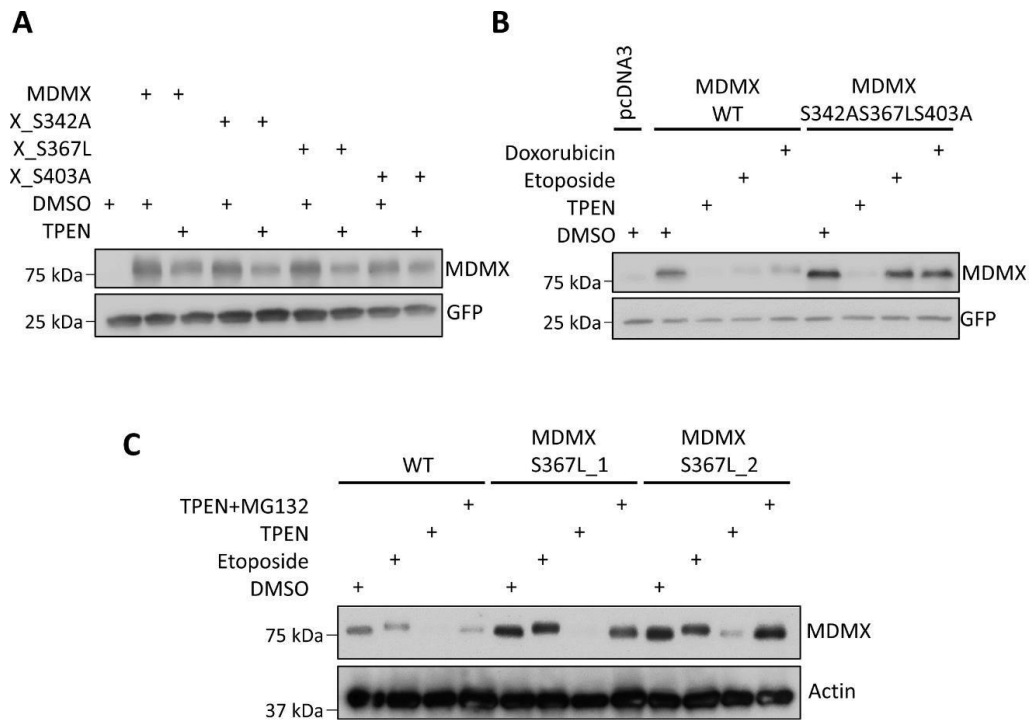
Figure II. 4. TPEN-induced MDMX reduction does not require MDMX phosphorylation at Ser342, Ser367, or Ser 403. (A) TPEN induces degradation of ectopically expressed MDMX variants S342A, S367L, or S403A. HEK293T cells were transfected with 0.15 µg of wild-type Myc-MDMX or Myc-MDMX variants S342A, S367L, or S403A. Twenty-four hours after transfection, the cells were treated with 5 µM TPEN for 8 hours. (B) MDMX mutant (S342AS367LS403A) is more resistant to etoposide or doxorubicin than TPEN treatment. MCF-7 cells in 60-mm dishes were transfected with 0.75 µg of wild-type Myc-MDMX or Myc-MDMX mutant (S342AS367LS403A). Six hours after transfection, the cells were trypsinized and plated into four 35-mm dishes. After 18 hours, the cells were treated with DMSO, TPEN (5 µM), etoposide (20 µM), or doxorubicin (10 µM) for 8 hours. (C) TPEN induces endogenous MDMX S367L degradation. U2OS cells with endogenous MDMX S367L mutation were treated with TPEN (5 µM), TPEN (5 µM) plus MG132 (20 µM), or etoposide (15 µM) for 8 hours.
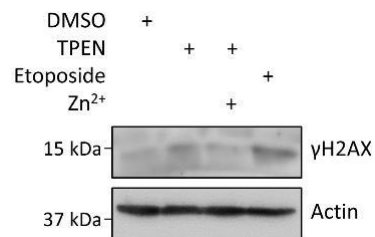
Figure II.S 4. TPEN induces DNA damage to a much lesser extent than etoposide. MCF-7 cells were treated with DMSO, 5 µM TPEN, or 15 µM etoposide for 8 hours. In one set of the TPEN treated cells, 25 µM ZnSO4 was added back 3 hours after TPEN treatment and the cells were incubated for another 5 hours. Total cell lysates were then prepared and subjected to immunoblotting with anti-γH2AX or anti-actin antibodies.

The ion channel protein TRPM7 interacts with MDMX and regulateszinc depletion-induced MDMX degradation

In a mass spectrometry-based proteomics analysis, we identified TRPM7, an ion channel protein, as a potential MDM2/MDMX heterodimer interacting protein (Figure II.S5A). Using co-immunoprecipitation assay with ectopically expressed proteins we confirmed itsinteraction with MDMX but not MDM2 (Figure II.S5B and II.S5C). Intriguingly, when weectopically expressed TRPM7 with MDMX in the presence or the absence of MDM2, we foundthat TRPM7 co-expression stabilized MDMX and induced a change in MDMX migration on SDS-PAGE (Figure II.5A). Since TRPM7 is a bifunctional protein with both ion channel and α-typekinase function (Runnels et al., 2001), we introduced either a channel-defective mutationE1047Q (M. Li et al., 2007) or a kinase-dead mutation K1646R (Schmitz et al., 2003) into TRPM7 and examined its effect on co-transfected MDMX. As shown in Figure 5B, the TRPM7E1047Q but not the TRPM7 K1646R was unable to stabilize MDMX or induce altered MDMXmigration on SDS-PAGE. Moreover, NS8593, a specific TRPM7 channel inhibitor (Chubanov,Schafer, Ferioli, & Gudermann, 2014), counteracted the effects of wild-type TRPM7 on MDMXstability and migration (Figure II.5C). Together, our results reveal that the channel function of TRPM7 is critical for TRPM7-induced MDMX stabilization and migration change on SDS-PAGE.

To further test if TRPM7 is involved in TPEN-mediated MDMX degradation, MCF-7 cells were transfected with control siRNA or two different siRNAs that targets TRPM7. Forty-eighthours later, cells were pre-treated with 5 µM TPEN and then 5 µM

ZnSO$_4$ was added. As shown in Figure 5D, Zn^{2+}-mediated recovery of MDMX in the presence of TPEN is attenuated upon the depletion of TRPM7. In line with this data, NS8593 attenuated the effect of Zn^{2+} on TPEN-induced MDMX degradation (Figure II.5E). On the other hand, we found that in TPEN-treated HEK293T cells, overexpression of TRPM7 facilitates the Zn^{2+}-mediated recovery of MDMX (Figure II.5F). Therefore, TRPM7 is likely involved in Zn^{2+}-mediated recovery of MDMX in TPEN-treated cells, which is most likely through its channel function.
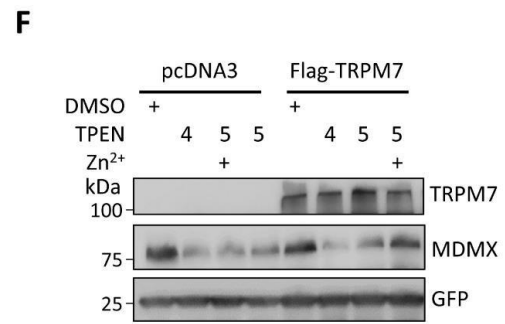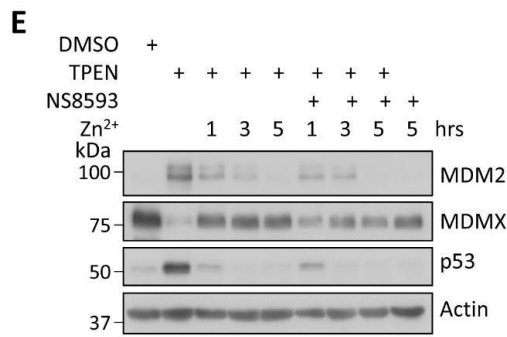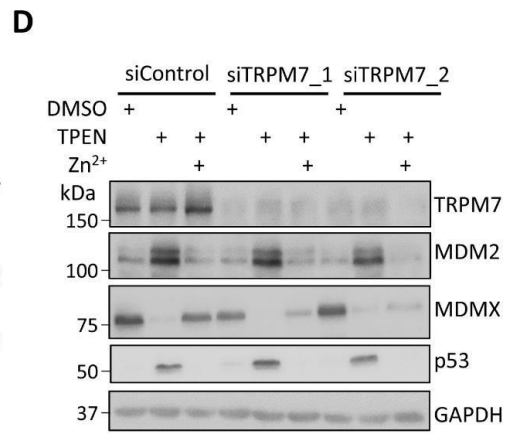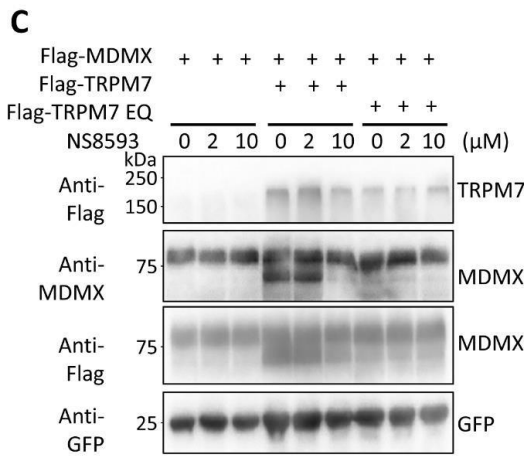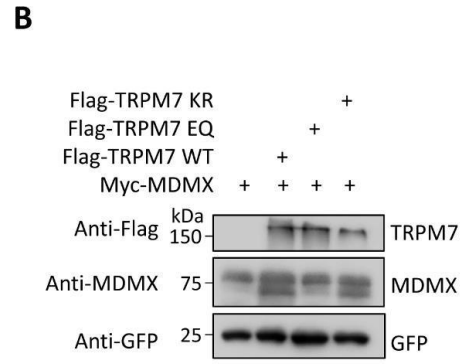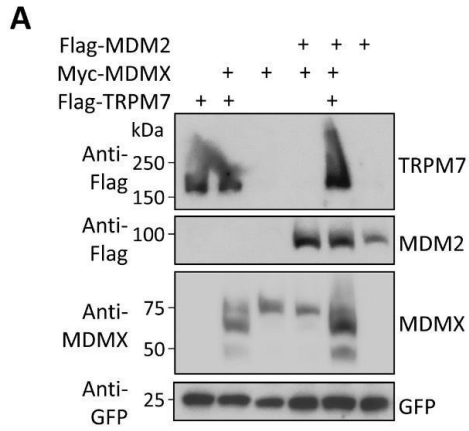
Figure II. 5. The ion channel protein TRPM7 stabilizes ectopically expressed MDMX, induces ectopic MDMX migration changes on SDS-PAGE, and regulates TPEN-induced MDMX degradation through its channel function. (A) TRPM7 stabilizes ectopically expressed MDMX and induces ectopic MDMX migration changes on SDS-PAGE. HEK293T cells were transfected with combination of Myc-MDMX (0.15 µg), Flag- MDM2 (1 µg), and Flag-TRPM7 (1 µg) as indicated. Total cell lysates were analyzed 24 hours after transfection. (B) Channel but not kinase function of TRPM7 is needed for TRPM7-induced MDMX migration change. HEK293T cells were transfected with Myc-MDMX (0.2 µg) and different Flag-TRPM7 variants (1 µg; wild-type, E1027Q or K1646R) as indicated for 24 hours. (C) TRPM7 channel inhibitor NS8593 counteracts the effect of wild-type TRPM7 on MDMX stability and migration change. HEK293T cells were transfected with Myc-MDMX (0.2 µg) and different Flag-TRPM7 variants (1 µg; wild-type, E1027Q or K1646R) as indicated. Twenty-four hours after transfection, DMSO or NS8593 (2 or 10 µM) was added and cells were incubated for another 12 hours before harvesting. (D) Knockdown TRPM7 by siRNAs attenuates Zn^{2+}- mediated recovery of MDMX in the presence of TPEN. MCF-7 cells were treated with control siRNA or two different siRNAs targeting TRPM7 (siTRPM7-1 and siTRPM7-2). Forty-eight hours later, the cells were treated with 5 µM TPEN for 5 hours and then incubated with or without 5 µM $ZnSO_4$ for another 5 hours. (E) TRPM7 channel inhibitor NS8593 attenuates Zn^{2+}-mediated recovery of MDMX in TPEN-treated MCF-7 cells. MCF-7 cells were treated with 5 µM TPEN for 5 hours and then 5 µM $ZnSO_4$ were added in the absence of presence of 50 µM NS8593. The cells were harvested at 1, 3 or 5 hours after $ZnSO_4$ and NS8593 treatment. (F) Overexpression of TRPM7 facilitates Zn^{2+}-mediated recovery of MDMX in TPEN-treated HEK293T cells. HEK293T cells were plated in 60 mm dishes and transfected with Flag-TRPM7 variants (2 µg). Twenty-four hours after transfection, cells were trypsinized and re-plated into three 35 mm dishes. Twenty- four hours after re-plating, the cells were treated with DMSO, 4 µM, or 5 µM TPEN for 5 hours. Then 5 µM $ZnSO_4$ was added into one of TPEN-treated dish. One hour later, the cells were harvested and total cell lysates were prepared and subjected to immunoblotting with anti-Flag, anti-MDMX, and anti-GFP antibodies.
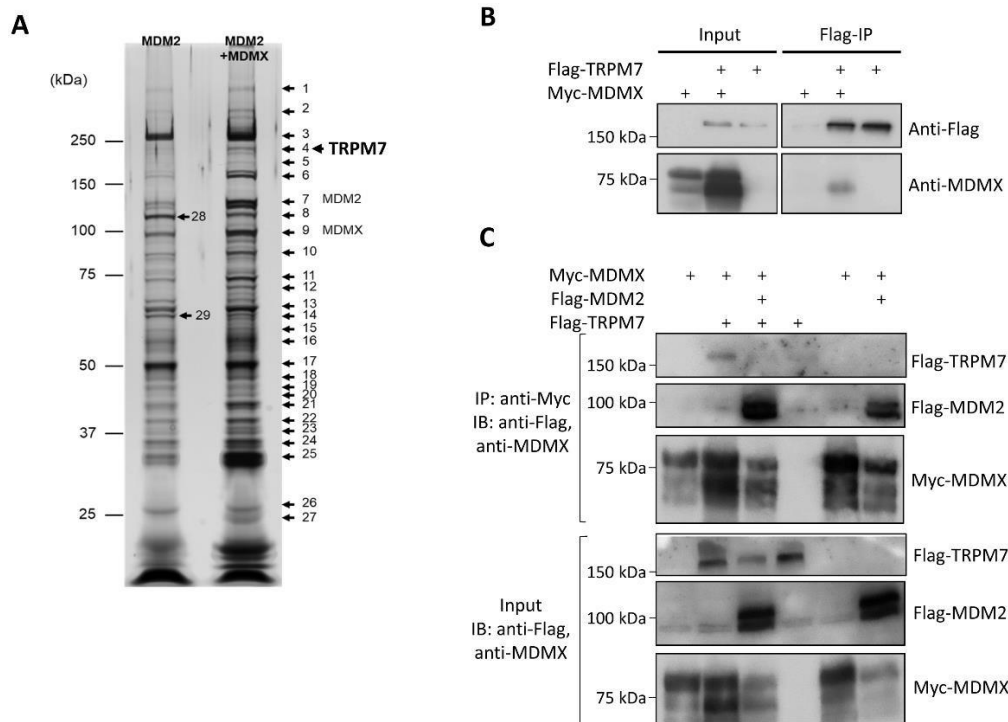
Figure II.S 5. TRPM7 interacts with MDMX. (A) TRPM7 was identified as a potential binding protein for MDM2/MDMX heterodimer. Twenty plates (150 mm) of HEK293T cells were each transfected with Flag- MDM2 (10 μg) or Flag-MDM2 (10 μg) plus Myc-MDMX (3 μg). Total cell lysates were prepared and subjected to immunoprecipitation with anti-Flag antibody. The co-immunoprecipitated proteins were analyzed by SDS-PAGE followed by silver staining. Differentially pulled-down protein bands were excised from the gel and subjected to mass-spectrometry analysis. Here, one protein in band 4 from co-immunoprecipitation samples of Flag-MDM2 plus Myc-MDMX co-transfected cells was identified as TRPM7. (B and C) TRPM7 interacts with MDMX. In Panel B, HEK293T cells were transfected with Flag-TRPM7 (1 μg), Myc-MDMX (0.3 μg) or in combination as indicated. Twenty-four after transfection, cells were harvested and total cell lysates were prepared and subjected to immunoprecipitation with anti-Flag antibody. The co-immunoprecipitated proteins were analyzed by immunoblotting with anti-Flag or anti-MDMX antibodies. In Panel C, HEK293T cells were transfected with Flag-TRPM7 (1 μg), Flag-MDM2 (1 μg), Myc-MDMX (0.3 μg) or in combination as indicated. Twenty-four after transfection, cells were harvested and total cell lysates were prepared and subjected to immunoprecipitation with anti-Myc antibody. The co-immunoprecipitated proteins were analyzed by immunoblotting with anti-Flag or anti-MDMX antibodies.

MDMX overexpression partially rescues the inhibitory effect of TPEN on cancer cell growth and the inhibitory effect of TRPM7 depletion oncancer cell migration

TPEN treatment inhibited MCF-7 cell growth on a colony formation assay, whereas the addition of zinc completely abolished the inhibitory effect of TPEN (Figure II.6A). TPEN treatment also repressed MCF-7 cell growth in a cell proliferation assay (Figure II.6B). NSC207895, an MDMX inhibitor that blocks the MDMX promoter and inhibits the MDMX expression (H. Wang, Ma, Ren, Buolamwini, & Yan, 2011), enhanced the inhibitory effect of TPEN on MCF-7 cell proliferation (Figure II.6B and Figure II.S6A). Similar results were obtainedusing MCF-7 cells treated with control siRNA or siRNA targeting MDMX in the absence or presence of TPEN (Figure II.S6B). On the other hand, using MCF-7 cells with tetracycline- inducible MDMX overexpression, we observed that the cells growing in the presence of tetracycline (a.k.a. with MDMX overexpression) were more resistant to the TPEN treatment inthe colony formation assay (Figure II.6C and Figure II.S6C). Together, these results indicated that MDMX protects MCF-7 cells from zinc depletion-mediated cell growth inhibition.

Previously it was reported that downregulation of TRPM7 in human cancer cells impairscell proliferation, migration, and invasion (Yee, 2017). As our data suggested that TRPM7 actively regulates cellular levels of MDMX, presumably through its channel function on intracellular zinc concentration modulation, we reasoned that MDMX overexpression might counteract the effect of TRPM7 inhibition on MCF-7 cells. Consistent with previous reports, depletion of TRPM7 using two different

siRNAs led to inhibition of MCF-7 cell growth in a colony formation assay (Figure II.6D). However, using MCF-7 cells with tetracycline-inducible MDMX overexpression inhibition of TRPM7 with either siRNAs (Figure II.S6D) or NS8593 (Figure II.S6E), we did not observe a cell growth difference for the cells with or without MDMX overexpression. Similarly, no cell growth difference was observed between MCF-7-Myc- MDMX cells with stably-expressed Myc-MDMX and MCF-7-pcDNA3 control cells (Figure II.S6F and II.S6G). Therefore, under our experimental conditions, MDMX overexpression does not rescue TRPM7 inhibition-mediated growth of MCF-7 cells.

We then assessed MCF-7 cell migration with a wound-scratch assay. As shown in Figure II.6E, we found that NS8593 treatment inhibited MCF-7 cell migration. Interestingly, MCF-7 cells with stably-expressed MDMX (Figure II.6E) or MCF-7 cells with tetracycline-induced MDMX overexpression (Figure II.S6H) were partially resistant to this inhibitory effect in comparison to control cells. Similarly, depletion of TRPM7 using siRNA inhibited MCF-7 cell migration while MCF-7 cells with stably-expressed MDMX (Figure II.6F) or MCF-7 cells with tetracycline-induced MDMX overexpression (Figure II.S6I) were partially resistant to this inhibitory effect in comparison to control cells. Together, our data indicate that TRPM7 may function through its regulation of MDMX to affect cell migration during tumorigenesis.

Figure II. 6. MDMX overexpression partially reverses the inhibitory effect of TPEN or TRPM7 inhibition on MCF-7 cell migration. (A) TPEN treatment inhibits MCF-7 cell growth in a zinc-dependent manner. 5×10^4 MCF-7 cells were plated on 35 mm dishes. Twenty-four hours later, the cells were treated with DMSO, TPEN (5 µM), or TPEN plus ZnSO4 (5 µM each) for 24 hours. Fresh DMEM medium was then added into each dish and replaced every other day. The cells were fixed and stained 5 days after treatment. (B) NSC207895 further inhibits TPEN-repressed MCF-7 cell proliferation. 1×10^4 MCF-7 cells were plated on 96-well plates and treated in triplicates with DMSO, TPEN (5 µM), NSC207895 (2.5 µM), or TPEN (5 µM) plus NSC207895 (2.5 µM) for 8 hours. Cell proliferation was measured as described in Materials and Methods. The results were expressed as means±s.d. of three independent experiments. (C) MDMX overexpression partially rescues the inhibitory effect of TPEN on MCF-7 cells. 5×10^4 MCF-7 cells with tetracycline-inducible MDMX overexpression were plated on 6-well plate with or without 2.25 µg/ml of tetracycline and treated with DMSO or 5 µM TPEN for 24 hours. Fresh medium was then added and replaced every other day. Five days later the cells were fixed and stained. (D) Knockdown of TRPM7 inhibits MCF-7 cell growth. MCF-7 cells were treated with control siRNA or siRNAs targeting TRPM7 (siTRPM7_1 and siTRPM7_2). Twenty-four hour after transfection, 2×10^4 cells were plated in 6-well plate and then fixed and stained 1 week later. (E) MDMX overexpression partially rescues cell migration repression mediated by NS8593. MCF-7-pcDNA3 and MCF- 7-Myc-MDMX cells were plated on 6-well plate to reach ~90% confluence. The cells were starved with DMEM plus 0.5% FBS for 24 hours. After that, the cells were scratched and incubated in DMEM plus 0.5% FBS with DMSO or NS8593 (30 µM). Images were taken at 0 or 24 hours after scratch. Percentage of healed wound area at 24 hours related to 0 hour time point was graphed. Representative data from one experiment were shown. (F) MDMX overexpression partially rescues cell migration repression mediated by TRPM7 ablation. MCF-7-pcDNA3 and MCF-7-Myc-MDMX cells were plated on 60 mm dishes for 24 hours and then transfected with control siRNA or siRNA targeting TRPM7 (siTRPM7_2). Six hours after transfection, 2×10^6 cells were plated in each well of a 6-well plate to reach ~90% confluence. The cells were starved with DMEM plus 0.5% FBS for 24 hours and then scratched. Images were taken and analyzed at 0 or 24 hours after scratch.
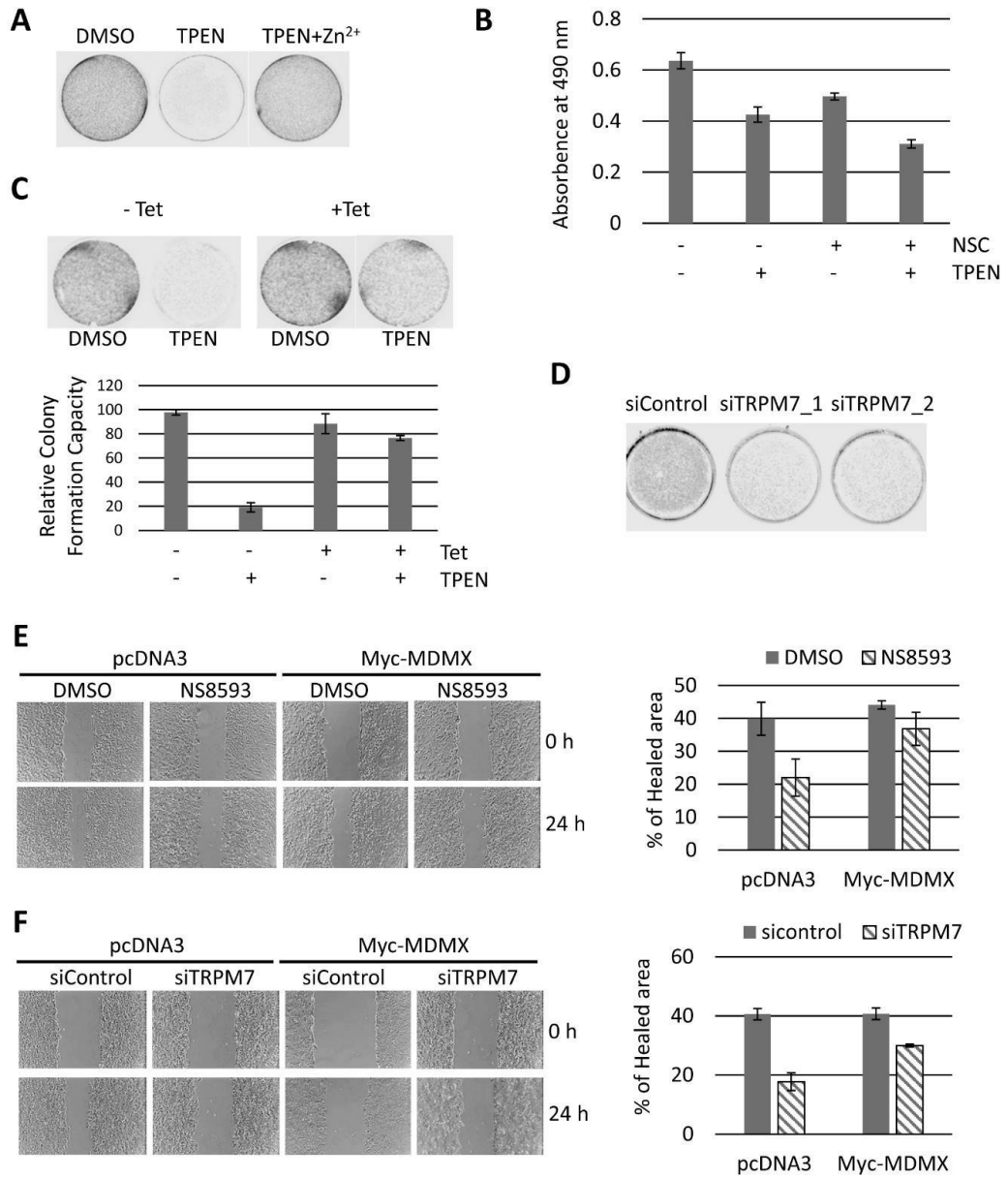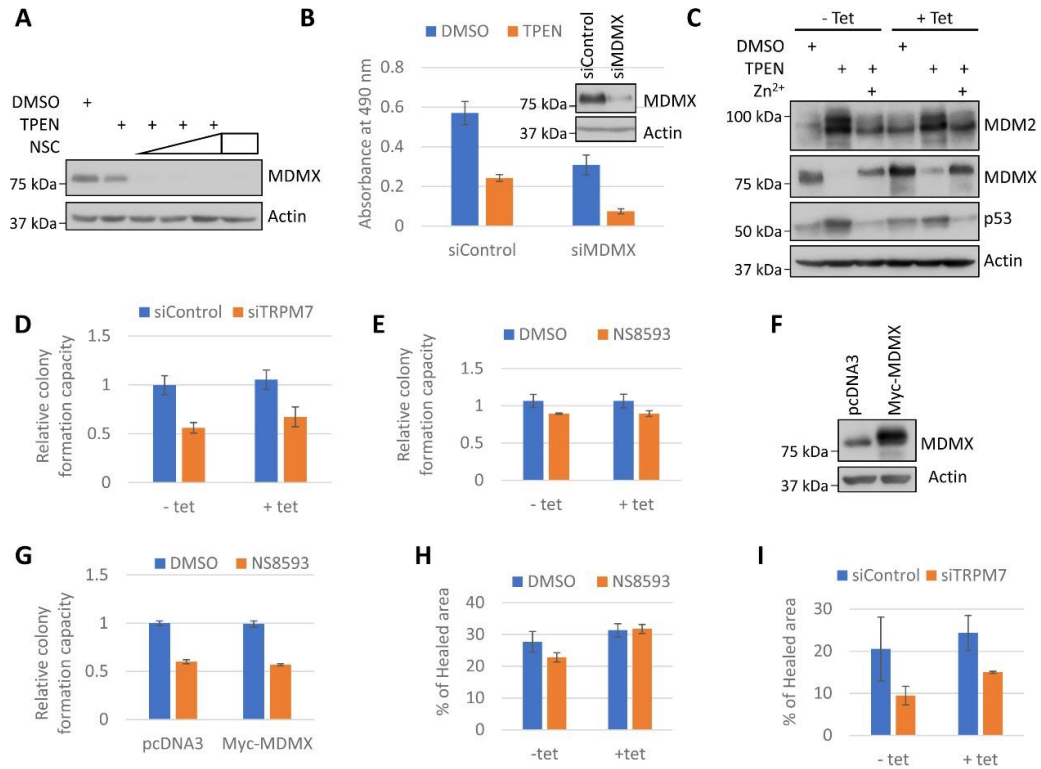
Figure II.S 6. MDMX over-expression partially reverses the inhibitory effect of TRPM7 inhibition on MCF7 cell migration. (A) NSC207895 inhibits MDMX expression in MCF7 cells. MCF7 cells were treated with DMSO, TPEN (5 µM), NSC207895 (NSC; 5 µM), or TPEN (5 µM) plus increasing dosages of NSC207895 (NSC; 1, 2.5 or 5 µM) for 8 hours. The cells were harvested and total cell lysates were prepared and subjected to immunoblotting with anti-MDMX and anti-actin antibodies. (B) Depletion of MDMX by siRNA further inhibits TPEN-repressed MCF-7 cell proliferation. MCF-7 cells were transfected with control siRNA or siRNA targeting MDMX (siMDMX). Eighteen hours later, the cells were trypsinized, counted, and plated (6×10^3 cells for each well) on 96-well plates in triplicates. After 24 hours, cells were treated with DMSO or TPEN (5 µM). Eight hours later, the medium was removed and replaced with 100 µl of fresh complete medium supplemented with 10 µl CellTiter 96® AQueous One Solution. After incubated for 1 hours at 37°C, the absorbance was measured on an TECAN SPARK Microplate Reader (Tecan) at a wavelength of 490 nm. The results were expressed as means±s.d. of three independent experiments. (C) Tetracycline induces MDMX expression in MCF7 cells with tetracycline inducible MDMX overexpression. MCF7 cells with tetracycline inducible MDMX overexpression were plated on 6-well plate with or without 2.25 µg/ml of tetracycline. Twenty-four hours later the cells were treated with DMSO or 5 µM TPEN. 5 µM ZnSO4 was added in one of the TPEN-treated cells 5 hours later. After another 5 hours incubation, the cells were harvested and total cell lysates were analyzed by immunoblotting with indicated antibodies. (D) MDMX overexpression does not rescue TRPM7 ablation-mediated cell growth inhibition. 5×10^4 MCF7 cells with tetracycline inducible MDMX overexpression were plated on 6-well plate in triplicates with or without 2.25 µg/ml of tetracycline. Twenty-four hours later the cells were transfected with control siRNA or siRNA targeting TRPM7 (siTRPM7_2). Fresh medium was added 6 hours after treatment and replaced every other day. Five days later the cells were fixed and stained with crystal violet (0.05% in 20% ethanol). The crystal violet stained cells were scanned using LI-COR Odyssey CLx imaging system. The intensity of crystal violet signal in each well was quantified to represent the cell

50

numbers in the well. The absorbance of control siRNA treated cells without addition of tetracycline was considered as 100%. (E) TRPM7 inhibitor NS8593 doesn't affect cell growth for tetracycline inducible MDMX overexpression MCF7 cell system. $5×10^4$ MCF7 cells with tetracycline inducible MDMX overexpression were plated on 6-well plate per well in triplicates with or without 2.25 µg/ml of tetracycline in the absence or presence of NS8593 (30 µM). Medium was replaced every other day. Five days later the cells were fixed and stained with crystal violet (0.05% in 20% ethanol). (F)MCF7-Myc-MDMX cells express higher levels of MDMX in comparison to MCF-pcDNA3 cells. MCF7- pcDNA3 and MCF7-Myc-MDMX cells were maintained in DMEM with 250 µg/ml G418. Total cell lysates were prepared and subjected to immunoblotting anti-MDMX and anti-actin antibodies. (G) TRPM7 inhibitor NS8593 doesn't affect cell growth for MDMX overexpression stable MCF7 cell system. $5×10^4$ MCF7-pcDNA3 and MCF7-Myc-MDMX cells were plated on 6-well plate in triplicates in the absence or presence of NS8593 (30 µM). Medium was replaced every other day. Five days later the cells were fixed and stained with crystal violet (0.05% in 20% ethanol). (H) MDMX over-expression partially reverses cell migration repression mediated by NS8593. MCF7 cells with tetracycline inducible MDMX overexpression were plated on 6-well plate with or without 2.25 µg/ml of tetracycline to reach ~90% confluence. The cells were starved with DMEM plus 0.5% FBS for 24 hours. After that, they were scratched and incubated in DMEM plus 0.5% FBS with DMSO or NS8593 (30 µM). Images were taken at 0 or 24 hours after scratch. Three different scratched areas were imaged and measured using MRI Wound Healing Tool. Percentage of healed wound area at 24 hours related to 0 hour time point was graphed. A representative data from one experiment were shown. (I) MDMX over-expression partially reverses cell migration repression mediated by TRPM7 knock-down. MCF7 cells with tetracycline inducible MDMX overexpression were plated on 60 mm dishes for 24 hours and then transfected with control siRNA or siRNA targeting TRPM7 (siTRPM7_2). Six hours after transfection both cells were trypsinized and counted. $2×10^6$ cells were plated in each well of a 6-well plate to reach ~90% confluence. The cells were starved with DMEM plus 0.5% FBS for 24 hours. After that, they were scratched and images were taken at 0 or 24 hours after scratch and analyzed as in (G). Representative data from one experiment were shown.

Discussion

Zinc conducts various biological roles and zinc deficiency has been linked to many humandiseases, including cancer development. MDMX, a zinc-containing protein and crucial negative regulator of p53, is amplified and/or overexpressed in various cancers. Here, we report for the first time that zinc depletion such as TPEN treatment results in MDMX degradation in a ubiquitination-independent and 20S proteasome-dependent manner. Moreover, we identified TRPM7, a zinc-permeable ion channel, as a novel MDMX-interactingprotein. TRPM7 inhibition by siRNAs or channel inhibitor NS8593 attenuates while TRPM7 overexpression facilitates the recovery of MDMX upon adding back of zinc to TPEN-treated cells. Most importantly, we found that TRPM7 inhibition suppresses breast cancer MCF-7 cell migration, which can be partially rescued by the overexpression of MDMX. In all, our data indicate that TRPM7 regulates cellular levels of MDMX in part by modulating intracellular zinc concentration. As such our findings with TRPM7 could suggest a therapeutic target for combinational cancer treatment.

In breast cancer patients it has been reported that zinc levels are lower in serum but are higher in breast cancer tissue than in normal breast tissue (Grattan & Freake, 2012). It is intriguing that breast cancer tissue has a significantly high uptake of zinc and it is unclear if these changes in serum and tissue zinc concentrations contribute to the initiation, promotion,or progression of breast cancer, or whether if they are the effects of malignant transformation. We observed that cellular levels of MDMX correlate with the intracellular zinc concentration.MDMX overexpression partially

rescues the inhibitory effect of zinc depletion on cell growth, indicating that zinc deficiency may impose selection pressure for cells with MDMX amplification or overexpression during breast cancer development.

Zinc affects the cellular levels of MDMX at the post-transcriptional level. Since MDMX isa zinc-containing protein with two zinc coordination motifs, we anticipated that zinc depletionleads to partially unstructured MDMX, which is subjected to 20S proteasome-mediated degradation. It is intriguing that MDM2, a well-known E3 ubiquitin ligase for both p53 and MDMX (Wade et al., 2013) that has also been shown to directly interact with the 20S proteasome and facilitate 20S proteasome-mediated p53 (Kulikov et al., 2010) or Rb (P. Sdeket al., 2005) degradation, is not involved in zinc depletion-mediated MDMX degradation. SinceMDM2 and MDMX bind to each other through their RING-finger domains, zinc depletion mayimpair their interaction by affecting the RING-finger structure. Further investigation will be needed to test if MDMX can bind to 20S proteasome by itself or if other unknown protein(s) are required for its 20S proteasome-mediated degradation.

Zinc transporters, zinc-permeable ion channels, and zinc-sequestering metallothioneins have been shown to be critical for intracellular zinc homeostasis. Deregulation of their function contributes to tumorigenesis (Kambe, Tsuji, Hashimoto, & Itsumura, 2015; Pan et al., 2017). Multiple zinc transporters (such as ZnT2, ZIP6/LIV1, ZIP7 and ZIP10), zinc-permeable ion channels (such as TRPC6, TRPM7, and TRPV6), as well as metallothionein were reported to be overexpressed in breast cancer, some of which are associated with breast cancer metastases and poor prognosis (Inoue,

O'Bryant, & Xiong, 2015).Relatedly, TRPM7 is abnormally overexpressed in various cancer cells including breast cancer(Yee, 2017) and knockdown of TRPM7 suppresses breast cancer cell migration and invasion (Middelbeek et al., 2012).

We had identified TRPM7 as a novel MDMX interacting protein and found that it both stabilizes MDMX and induces changed migration of the MDMX on SDS-PAGE when the two proteins are ectopically co-expressed. Although the functional importance of this migration change of MDMX remains unknown, we found that the channel domain but not the kinase domain is essential for the MDMX migration change under our experimental condition. Importantly, we observed that overexpression of TRPM7 facilitates but TRPM7 ablation or NS8593 treatment inhibits the recovery of cellular levels of MDMX after adding back zinc to TPEN-treated cells. Therefore, TRPM7 actively regulates cellular levels of MDMX, most likely through its zinc permeable channel function. Moreover, we further demonstrated that suppression of MCF-7 cell migration upon the inhibition of TRPM7 can be partially rescued by MDMX overexpression. Based on these findings, we speculate that overexpression of TRPM7in breast cancer cells raises their intracellular zinc concentration, which, in turn, increases cellular levels of MDMX to promote cancer cell migration. As the cleaved C-terminal kinase domain of TRPM7 has other activities in the nucleus (Krapivinsky et al., 2014), it is very likely that other mechanism(s) are employed by TRPM7 to promote breast cancer progression. Future investigations will be needed to explore those mechanisms.

TRPM7 is not unique among proteins that are relevant to zinc biology in regards

to breast cancer. Other zinc-permeable ion channels, zinc transporters, as well as

metallothioneins may employ similar mechanisms to influence breast cancer

development by modulating the cellular levels of zinc and MDMX levels. Indeed,

when we knocked down ZIP7, a zinc transporter that is overexpressed in breast

cancer, we observed similarly attenuated MDMX recovery in TPEN-treated MCF-7

cells upon adding back zinc (Figure II.S7). Therefore, modulating the intracellular

zinc concentration may be an effective therapeutic strategy for cancer treatment.

Depending on cellular levels of MDMX and TRPM7 as well as other proteinsinvolved in

zinc homeostasis, therapeutic strategies and zinc supplementation guidelines have

potential for development as cancer therapeutics, diagnosis or prevention.
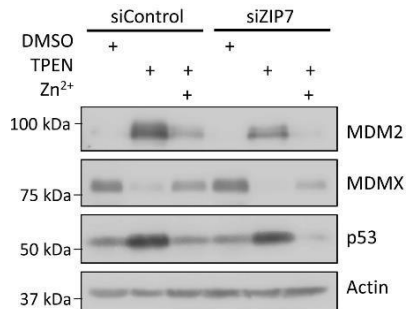
Figure II.S 7. Ablation of Zip7 attenuates Zn2+-mediated recovery of MDMX in the presence of TPEN. MCF7 cells were treated with control siRNA or siRNA targeting Zip7. Forty-eight hours later, cells were treated with 5 µM TPEN for 5 hours and then treated with or without 5 µM ZnSO4 for another 5 hours. The cells were harvested and total cell lysates were analyzed by immunoblotting with indicated antibodies.

Experimental procedures

Cell culture and plasmids

Hek293T, U2OS, and MCF-7 cells were cultured in DMEM medium with 10% FBS (Fetal Bovine serum, Gemini Bio-products) and 1% penicillin-streptomycin (Gibco) at 37°C, 5% CO_2. For zinc-deficient DMEM medium, FBS was incubated overnight with 5% Chelex 100 (Bio-Rad) before supplemented (10%) into DMEM medium. MCF-7-pcDNA3 and MCF-7-Myc-MDMX celllines were constructed by transfecting pcDNA3 or Myc-MDMX plasmid into MCF-7 cells and then selecting G418 (1mg/ml) resistant clones for 2 weeks. Pooled cell clones were maintained in DMEM with 250 µg/ml G418. MCF-7 with tetracycline-inducible MDMX cell line was obtained from Dr. Xinbin Chen (University of California Irvine) and was maintained in DMEM with 4 µg/ml Blasticidin and 25 µg/ml Zeocin. U2OS MDMX S367L mutant cells were generated using CRISPR/Cas9 genome-editing technology (Cong et al., 2013) as described in Supplemental Material.

HA-p53, Flag-MDM2, Myc-MDMX, and His-Ubiquitin were described previously (Zhu et al., 2009). Flag-TRPM7 was a kind gift from Dr. Clapham (Howard Hughes Medical Institute). Myc-MDMX variants (S342A, S367L, S403A, and D361A) and Flag-TRPM7 variants (E1047Q and K1646R) were constructed by site-directed mutagenesis. All the mutations were confirmed by Sanger sequencing.

Antibodies and reagents

Commercially obtained antibodies used were as follows: MDMX (A300-287A,

Bethyl; or 8C6, Millipore), actin (C-4, Santa Cruz Biotechnology), Flag (M2, Sigma), HA (HA.11, Covance), TRPM7 (A302-700A, Bethyl) and GFP (B-2, Santa Cruz Biotechnology). Mouse monoclonal antibodies against human p53 (DO-1) and MDM2 (3G5, 4B11, 5B10) were used as supernatants from hybridoma cultures. Reagents used in this study were as follows: TPEN (N ,N , N', N'-tetrakis (2-pyridinylmethyl) - 1,2-ethanediamine), MG132, CaCl$_2$, MgCl$_2$, and ZnSO$_4$ from Sigma; NS8593, bispicen, chloroquine, bafilomycin A1, capzimin dimer, Z-VAD- FMK, and NSC207895 from Calbiochem.

Transfections

Plasmid transfections were performed using PEI (Polysciences; cat# 23966-2) for HEK293T cells and Lipofectamine 2000 (Thermo Fisher Scientific) for MCF-7 cells. siRNA transfections in MCF-7 cells were performed using Dharmafect 1 (Dharmacon) using 50 nM of control siRNA (Allstar negative control siRNA; Qiagen) or siRNA targeting TRPM7, MDM2 or Rpn2. The target sequences are: 5'-TTAATGTATCTACCGTCAGGG-3' (siTRPM7_1), 5'- GAGTATTTCATGGCAAGAC-3' (siTRMP7_2), 5'-AAGCCATTGCTTTTGAAGTTA-3' (siMDM2_1), 5'-AAGGAATAAGCCCTGCCCA-3' (siMDM2_2). 5'-GTCTAGATGATCACAAGTA-3' (siRpn2_1) and 5'-GGGTGTAATTCATAAGGGT-3' (siRpn2_2).

RNA extraction and quantitative RT-PCR analysis

RNA was extracted using a Qiagen RNeasy mini-kit, and cDNA was synthesized with the QuantiTect reverse transcription kit (Qiagen). Samples were analyzed by

quantitative real-timePCR on a Bio-Rad CFX 96 using PowerUp SYBR Green (Thermo Fisher Scientific). RNA expression was normalized to RPL32 mRNA expression. Relative levels were calculated by thecomparative Ct method ($\Delta\Delta C_T$ method). The results are expressed as means±s.d. of four experiments. Primer sequences are: RPL32, 5'-TTCCTGGTCCACAACGTCAAG-3'(Forward) and 5'-TGTGAGCGATCTCGGCAC-3' (Reverse); MDMX, 5'-GCAAGAAATTTAACTCTCCAAGCAA-3' (Forward) and 5'-CTTTGAACAATCTGAATACCAATCCTT-3' (Reverse).

In vivo ubiquitination assay

In vivo ubiquitination assays were carried out using a His-Ub construct. After cells were harvested, a Ni-NTA pull-down assay was carried out as previously described (Zhu et al., 2009).Eluted proteins were analyzed by Western blotting with anti-MDMX or anti-p53 antibody.

Cell proliferation assay

Cell proliferation was measured using the CellTiter 96® AQueous One Solution Cell Proliferation Assay (Promega) following manufacturer's instruction. 1×10^5 MCF-7 cells per wellwere plated in 96-well plates. The cells in triplicates were then treated as indicated and the plates were read on a TECAN SPARK Microplate Reader (Tecan) at a wavelength of 490 nm. The results were expressed as means±s.d. of three independent experiments.

Colony formation assay

5×10^4 MCF-7 cells (on 35 mm dishes), MCF-7 with tetracycline inducible MDMX overexpression (on 6-well plate with or without 2.25 µg/ml of tetracycline), or MCF-7 transfected with siRNA targeting TRPM7 (on 6-well plate 6 hours after transfection) were plated. The cells were treated with indicated drugs for 24 hours and then fresh DMEM mediumwere added and replaced every other day. Five to seven days after treatment the cells were fixed and stained with crystal violet (0.05% in 20% ethanol).

Wound Healing Assay

About 2×10^6 cells MCF-7 were plated (for experiments with TRPM7 depletion, MCF-7 cells were plated 6 hours after siRNA transfection) to reach ~90% confluence, the cells were starved with DMEM plus 0.5% FBS for 24 hours. Then the cells were washed twice with 1×PBS, scratched with a 200-µL pipette tip to produce a straight cell-free "wound", and washed againwith 1×PBS to remove debris followed by addition of fresh DMEM plus 0.5% FBS DMEM withDMSO or NS8593 (30 µM) as indicated. Images were taken at 0 or 24 hours after scratch usinga phase-contrast microscope (Nikon, Eclipse Ts2) with 10× magnification. The healing areas were measured using MRI Wound Healing Tool (http://dev.mri.cnrs.fr/projects/imagej-macros/wiki/Wound_Healing_Tool) in Image J. Three different scratched areas for each dish/well were imaged and measured. Percentage of healed wound area at 24 hour related to0 hour time point was graphed as Percentage of healed area = (area 0h - area 24h)/area 0h ×100%.

Supporting information

Materials and Methods

Cell culture and plasmids

HEK293T cells, PC3 cells and MCF-7 cells were cultured in DMEM medium with 10% FBS (Fetal Bovine serum, Gemini Bio-products) and 1% penicillin streptomycin (Gibco) at 37°C,5% CO2. LNCaP cells were cultured in RPMI medium with 10% FBS (Fetal Bovine serum, GeminiBio-products) and 1% penicillin streptomycin (Gibco) at 37°C, 5% CO_2. MCF-7-pcDNA3 and MCF-7-Myc-MDMX cell lines were maintained in DMEM with 250 μg/ml G418. MCF-7 with tetracycline inducible MDMX cell line was maintained in DMEM with 4 μg/ml Blasticidin and 25 μg/ml Zeocin.

To establish U2OS MDMX S367L mutant cells, the left (anti-sense; GGAAGGTTTCTGAAAGGAAGTAC) and right (sense; CAAATCCTAGGCTAGATCACTGG) sgRNAs were cloned into pX335 (Addgene #42335) to cut the genome DNA in the intron 10 of mdmxgene. Donor vector was designed to introduce mutation S367L (TCG to TTG) in exon 11 of mdmx gene with a FNF selection cassette flanked by left and right homologous arms and cloned into pFNF (Addgene #22687). The donor and CRISPR plasmids were transfected into U2OS cells, followed by selection with G418 (800 μg/ml) for 2 to 3 weeks. The resistant cloneswere expanded and examined for FNF insertion on the mdmx locus by PCR. The corrected clones were confirmed by both genome and cDNA sequencing. To serve as controls, isogenicwild-type clones were also obtained through the same selection process. We obtained two

heterozygous (#12, S367L_1; #20, S367L_2) and one homozygous (#23, S367L_3) CRISPR cell lines. As the homozygous cell line was somewhat unstable and expressing much less MDMX,we only used the two heterozygous cell lines in this study.

Antibodies and reagents

Antibodies and reagents that were used only in supplemental data section are: phosphor-Histone H2A.X (Ser139) (20E3; Cell Signaling Technology); PARP (9542; Cell Signaling Technology); LC3B (NB100-2220; Novus); HLI373 (Sigma); Compound 1 (Sigma); MD-224 (30 nM, MedChem Express); Etoposide (Sigma); Zip7 siRNA (sc-76962; Santa Cruz Biotechnology);siMDMX (Hs_MDM4_4 FlexiTube siRNA; Qiagen).

ROS detection assay

2.2×10^4 MCF-7 cells per well were plated in triplicates for 5 experimental groups on 96-well plate. Eighteen hours later, two sets of triplicate cells were treated with DMSO or TPEN(5 µM) for 8 hours and cellular ROS levels were measured using ROS Detection Cell-Based Assay Kit (DCFDA) (item 601520; Cayman Chemical) following the manufacture's procedure. 10 µM of DCFDA was used in the assay for MCF-7 cells. Positive control (pyocyanin treatment),negative control (N-actyl cysteine treatment), and no treatment control were also included for measurement in triplicates. Total DCFDA (2,7-Dichlorofluoroscin Diacetate) fluorescence was measured using an excitation wavelength at 480 nm and emission wavelength at 530 nm.

Purification of MDM2 or MDM2/MDMX Complex and mass spectrometry

HEK293T cells were transfected with Flag-MDM2 or Flag-MDM2 plus Myc-

MDMX. Potential differential binding partners for MDM2 alone or MDM2/MDMX heterodimer were purified and subject to mass spectrometry analysis as previously described. Briefly, the HEK293T cells (1 x 10^10) were transfected with a Flag-MDM2 or Flag-MDM2 plus Myc-MDMX at a ratio of 10:3. Total cell lysates were prepared and subjected to immunoprecipitation withanti-FLAG monoclonal antibody (M2)-conjugated beads (Sigma-Aldrich, St. Louis, MO). The beads were washed eight times with lysis buffer and then eluted by incubating with 0.2 mg/mlFLAG peptide (Sigma-Aldrich) for 2 hrs. The eluate was concentrated and separated on a Tris-Glycine gradient gel (4-20%). Proteins on the gel were stained with GelCode Blue (Thermo Fischer Scientific, Waltham, MA). Differentially pulled-down protein bands were excised, destained with 25 mM ammonium bicarbonate and 50% acetonitrile, dried, digested with sequence grade modified trypsin (Promega, Fitchburg, WI) in 50 mM Tris-HCl [pH 7.6], extracted with 5% trifluoroacetic acid (TFA), 50% acetonitrile, and subjected to MALDI-TOF mass spectrometry analysis.

Chapter III. Detection of cytokine receptors using tyramide signal amplification for immunofluorescence

Abstract

Tyramide signal amplification (TSA) is an enzyme-mediated method to enhance the immunohistochemical detection of protein, nucleic acid, or other molecules in situ.

Here we describe immunofluorescent detection of a low abundance cytokine receptor, interleukin-17 receptor B (IL17RB) in U2OS cells, using tyramide signal amplification. In addition, we present a tyramide signal amplification compatible double-color immunostaining protocol using primary antibodies from same host species. Those applications allow detection of cellular proteins with enhanced sensitivity and add flexibility on primary antibody selection in double or multicolor immunofluoresence staining assays.

Introduction

Tyramide signal amplification (TSA) utilizes the catalytic activity of horseradish peroxidase (HRP) to deposit of a labeled (e.g., fluorophore, biotin, or other labeling moieties) tyramide onto target proteins that are previously blotted with primary antibody or nucleic acid sequences in-situ. In TSA-based immunohistochemical (IHC) or immunofluorescence (IF) detection, activated tyramide forms covalent bonds with tyrosine residues on the target protein, resulting in permanent high density labeling. The signals can then be detected by standard chromogenic or fluorescent techniques. As this technique is based on detection via indirect immunostaining involving primary and secondary antibodies, TSA promotes enhanced sensitivity and high specificity for target protein detection, especially for those low abundance proteins.

Double or multicolor immunofluoresence staining is useful to examine the distribution of two (or more) different antigens in the same sample of cells. It requires unlabeled primary antibodies from different hosts or different fluorescently labeled primary antibodies for different antigens. The availability of primary antibodies restricts the usage of the application. TSA-based covalently linked labeling can preserve antigen-associated signal even after serial stripping of the primary/secondary antibody pairs, making this process amenable to multiple rounds of staining in a sequential fashion (Hunyady, Krempels, Harta, & Mezey, 1996; Parra et al., 2017; Stack, Wang, Roman, & Hoyt, 2014). Most importantly, immunostaining with tyramide signal amplification allows double or multicolor

immunofluoresence staining being performed using unlabeled primary antibodies from same hosts without the concern for crosstalk. This will add flexibility on the primary antibody selection and facilitate multiplex staining design.

Il17RB is a cytokine receptor that binds to interleukin 17 (IL-17) cytokine family members IL-17B and IL-17E (IL-25) (Monin & Gaffen, 2018). It has been detected in kidney, pancreas, liver, brain, and intestine (Kolls & Linden, 2004). Amplification of IL-17B/RB signaling has been linked to tumorigenesis in breast (Alinejad, Dolati, Motallebnezhad, & Yousefi, 2017), gastric (Bie et al., 2017), pancreatic (Wu et al., 2015), and thyroid (Ren, Xu, Liu, Wang, & Qin, 2017) cancers. We have observed that low levels of IL17RB expression in using tyramide signal amplification for immunofluorescence (Figure III.1). In addition, we describe a tyramide signal amplification compatible double-color immunostaining protocol using primary antibodies against IL17RB and p53, a tumor suppressor, from the same host species (Figure III.2).
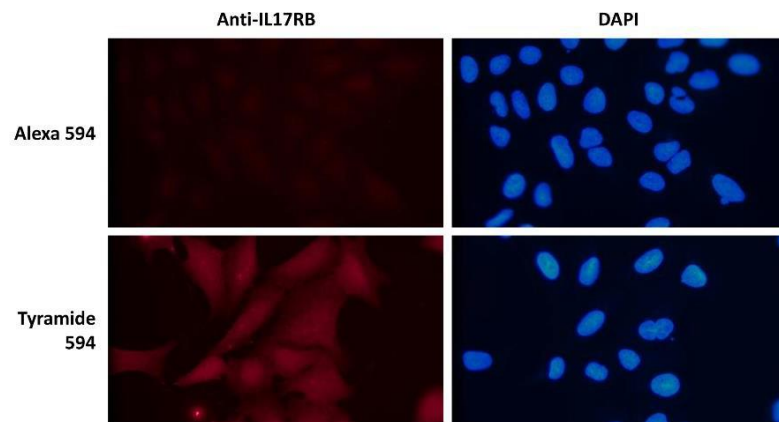
Figure III. 1. Tyramide signal amplification allows the detection of low abundance cytokine receptor IL17RB. Immunofluorescence staining of IL17RB in U2OS cells with goat anti-rabbit IgG (H+L) Alexa Fluor™ 594 secondary antibody. Immunofluorescence staining of IL17RB in U2OS cells with Alexa Fluor™ 594 Tyramide SuperBoost™ Kit, goat anti-rabbit IgG.
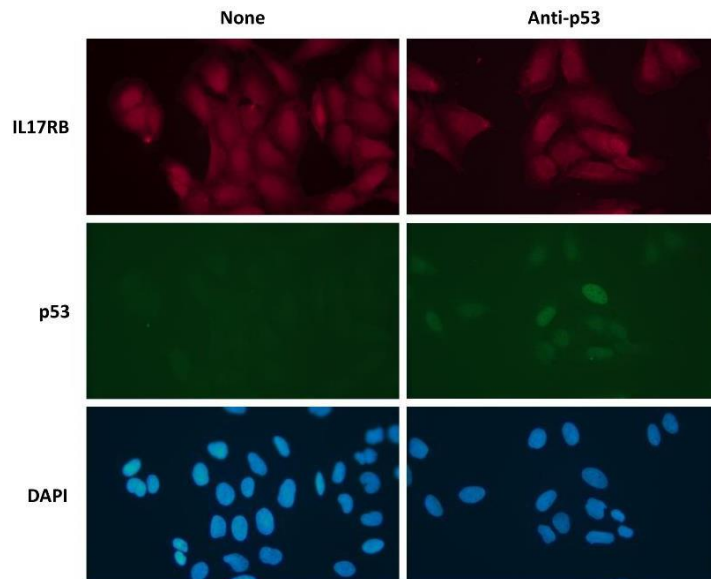
Figure III. 2. Tyramide signal amplification allows the double-color immunostaining of IL17RB and p53 using primary antibodies from the same host species. IL17RB in U2OS cells was stained with Alexa Fluor™ 594 Tyramide SuperBoost™ Kit, goat anti-rabbit IgG followed by immunostaining of p53 with goat anti- rabbit IgG (H+L) Alexa Fluor™ 488 secondary antibody. Primary antibodies against IL17RB and p53 are both rabbit polyclonal antibodies.

Materials

All reagents and solutions are stored according to the manufacturer's instructions.

Cell culture

1. Human osteosarcoma U2OS cells.

2. DMEM complete medium: Dulbecco's Modified Eagle Medium supplemented with 10% Fetal Bovine Serum and 100 µg/mL penicillin/streptomycin.

3. 1X Phosphate-buffered Saline (PBS, pH 7.2): 140 mM NaCl, 2.6 mM KCl, 2 mM Na_2HPO_4, 1.45 mM KH_2PO_4.

4. 4% paraformaldehyde in 1X PBS (*see* **Note 1**).

5. Alexa Fluor™ 594 Tyramide SuperBoost™ Kit, goat anti-rabbit IgG (*see* **Note 2**).

6. Antibodies: anti-p53 (FL393; Santa Cruz); anti-IL17RB (NBP2-43767; Novus); Goat anti- rabbit IgG (H+L) Alexa Fluor™ 594 secondary antibody; Goat anti-rabbit IgG (H+L) Alexa Fluor™ 488 secondary antibody.

7. Blocking buffer: 0.5% BSA in 1X PBS.

8. Permeabilization buffer: 0.5% Triton X-100 in 1X PBS.

9. 10 mM sodium citrate (pH 6.0): fleshly made from 1 M sodium citrate (pH 6.0) stock.

10. 5 mg/mL DAPI in DMSO.

11. Fluorescence microscope (Nikon Eclipse Ti2).

12. Cell culture dishes: diameter 35 mm.

13. Cover slides: 22 x 22mm.

14. Microscope slides: 75 x 25mm.

15. Microwave-safe container: about 76 x 150 mm (*see* **Note 3**).

16. Microwave.

17. CO_2 incubator: set to 5% CO_2 and 37 ºC.

Method

Immunofluorescent staining with tyramide signal amplification

1. Perform cell culture procedures in biosafety cabinets using sterile equipment and pre-warmed (37 ºC) reagents.

2. The day before immunostaining, place sterile glass coverslips in each 35 mm cell culture dish using sterile forceps.

3. Seed 6 x 105 U2OS cells into each 35 mm dish with glass coverslips.

4. Incubate the cells with 2 ml DMEM in a 37 ºC CO_2 incubator.

5. On the second day, aspirate the DMEM medium from the dish and wash the cells twice with 1 ml 1X PBS at room temperature.

6. Fix cells with 1 ml 4% paraformaldehyde in 1X PBS, at room temperature for 20 minutes.

7. Wash the cells with 1X PBS.

8. Permeabilize the cells with permeabilization buffer at room temperature for 90 seconds.

9. Wash the cells with 1X PBS.

10. Block the cells with blocking buffer at room temperature for 20-30 minutes.

11. Incubate the cells with the 100 ul anti-IL17RB antibody (1:500 dilution in blocking buffer) at room temperature for 1 hour (*see* **Note 4**).

12. Wash the cells 3 times with 1X PBS.

13. Incubate the cells with the anti-rabbit second antibody with HRP at room temperature for 2 hours (*see* **Note 5**).

14. Wash the cells 3 times with 1X PBS.

15. Prepare the following solutions during washing (*see* **Note 6**):

    a. 100X H_2O_2: one drop (50µL) of stock (3%) to 1 ml distilled water

    b. 1X Reaction Buffer (RB): one drop of stock to 1 ml distilled water

    c. Stop solution: 1:11 dilution in 1X PBS (10 ul stock in 100 ul 1X PBS)

16. Prepare the tyramide solution by mixing 100 ul of 1XRB + 1 ul of 100XH2O2 + 1 ul of Tyramide stock (*see* **Note 7**). Mix the solution by briefly vortexing.

17. Add the tyramide solution to the cells on and incubate them in the dark for 5 minutes (*see* **Note 8**).

18. Add the 100 ul stop solution to the cells and wash them using 1X PBS.

19. Counter stain cells with 0.5 µg/mL DAPI (freshly diluted in 1X PBS) for 1 minutes.

20. Wash the cells 3 times using 1X PBS.

21. Mount the cover slip onto a frosted microscope slide preloaded with 9 ul cold 50% glycerol.

22. Seal the cover slips with nail polish (fix the corners first and then spread it to all the edges).

23. Incubate for 15 min at room temperature in the dark to allow the nail polish to dry.

24. Store the cover slips in a dark place at 4°C in a slide box.

25. Double-color immunofluorescent staining with tyramide signalamplification

Double-color immunofluorescent staining with tyramide signal amplification

1. Perform procedures as in section 3.1, steps 1-17 to immunostain IL17RB with tyramide signal amplification.

2. Wash the cells 3 times using 1X PBS.

3. Aliquot 40 ml sodium citrate into a microwave-safe container and microwave at Hi power for 1 minute with cap on (*see* **Note 9**).

4. Take out the cover glass from 35 mm dish with thin-tipped forceps, place it (the cell side up) in the heated the sodium citrate solution, and microwave at Hi power for 30 seconds (*see* **Note 10**).

5. Take out the cover glass from the container and put it back into 35 mm dish with 1X PBS.

6. Wash the cells 3 times with 1X PBS.

7. Block the cells with blocking buffer at room temperature for 20-30 minutes.

8. Incubate the cells with the 100 ul anti-p53 antibody (1:500 dilution in blocking buffer) at room temperature for 1 hour in the dark.

9. Wash the cells 3 times with 1X PBS.

10. Incubate the cells with the100 ul goat anti-rabbit IgG (H+L) Alexa Fluor™ 488 secondary antibody (1:200 dilution in blocking buffer) at room temperature for 1 hour in the dark.

11. Wash the cells 3 times with 1X PBS.

12. Counter stain them with 0.5 µg/mL DAPI (freshly diluted in 1X PBS) for 1 minutes.

13. Wash the cells 3 times using 1X PBS.

14. Mount the cover slip onto a frosted microscope slide preloaded with 9 ul cold 50% glycerol (*see* **Note 11**).

15. Seal the cover slips with nail polish (fix the corners first and then spread it to all the edges).

16. Incubate for 15 min at room temperature in the dark to allow the nail polish to dry.

17. Store the cover slips in a dark place at 4°C in a slide box.

Fluorescence microscopy

1. Place the microscope slides containing coverslips (with the coverslips facing down) on the Nikon Eclipse Ti2 fluorescence microscope.

2. Obtain all images with a 50X fluorescent oil objective using 470 (green), 590 (red), and DAPI (blue) channels.

3. Adjust the exposure time and light intensity to obtain an optimum contrast between the signal and the background fluorescence. Use the same setting to take images for all the slides (*see* **Note 12**).

Notes

1. Paraformaldehyde is toxic and hard to dissolve. To make 4% paraformaldehyde 50 mL in 1X PBS:

a. Add 2 g of paraformaldehyde to 40 mL 65°C ddH2O.

b. Add 150μL of 1M NaOH (or 30μL of 5 M NaOH) to help paraformaldehyde dissolve faster. Mix the solution until it is clear and all the paraformaldehyde has dissolved

c. Add 5 mL of 10X PBS.

d. Adjust the pH of solution using 1M HCl to 7.2

e. Add ddH$_2$O to bring the volume to 50 mL.

f. Filter the solution using 45 um filter. The solution can be store at 4°C for up to 3 days. For long term storage, an aliquot of the solution should be kept at -20°C.

2. There are tyramide signal amplification from different vendors. SuperBoost kit is used in the present protocol because it has 2-10 times greater sensitivity than regular tyramide amplification techniques. Depending on the availability of antibody and choice of Alex Fluor dye, different kit can be used. In kit it contains 1X blocking buffer, 1X poly-HRP-conjugated secondary antibody, Alexa Fluor tyramide reagent, stabilized 3% hydrogen peroxide solution, 20X reaction buffer, reaction stop solution, and dimethylsulfoxide (DMSO). Please see manufacturer's brochure for details.

3. Any microwave-safe container can be used. Based on the size of container, the volume of sodium citrate and microwave time need to be adjusted to make sure that the sodium citrate buffer is boiled and the cover glass is immersed in the buffer all the time.

4. Depending on the primary antibody used, 1 hour room temperature or 4°C overnight primary antibody incubation can be performed. For overnight incubation, a humidified chamber such as a covered box with damp paper towel is needed to avoid sample dry out.

5. Anti-rabbit second antibody with poly-HRP from the SuperBoost kit is used here. In this system, several HRP enzymes are conjugated with short polymers to enhance the signal over regular HRP system. The optimal incubation time is 2 hours but it can

be adjusted to achieve the best specific signal/background signal ratio.

6. 100X H2O2, 1X Reaction buffer, and Stop solution need to be prepared fresh. The reaction stop reagent stock solution is prepared according to manufactures' instruction and stored at -20°C.

7. 100X Tyramide stock solution: the Alexa Fluor tyramide reagent is dissolved in DMSO according to manufactures' instruction and stored at 4°C in dark. Depending on the choice of Alex Fluor dye, a SuperBoost kit with a specific Alexa Fluor tyramide reagent is needed.

8. Incubation time can be adjusted to achieve the best specific signal/background signal ratio. Five minutes incubation works for most of the applications in our hand.

9. For a microwave safe container with size about 76 x 150 mm, 40 mL sodium citrate is optimal for the application. Based on the container used, the volume of sodium citrate need to be adjusted. In addition, since different microwave oven models have different power setting, the microwaving time need to be adjusted accordingly. The sodium citrate buffer need to be boiled before putting in the coverslip. The coverslip need to be immersed in the buffer all the time during the microwaving.

10. The microwaving time need to be adjusted depending on different microwave oven models to keep the buffer in boil but not dry. For tissue samples, it has been suggested to place the sample in citrate buffer and heat with 100% power until boiling and then reduce the power to 20% and keep microwaving for additional 15 minutes.

11. A mountant with antifade properties is preferred but cold 50% glycerol is OK for normal use.

12. Depending on the signal observed from fluorescence microscopy, adjustment can be made for immunostaining steps. If there is low signal, primary antibody dilution and incubation time can be optimized. Also, the incubation time with tyramide reagent for step 3.1.17 can be lengthened. If there is excess signal, primary antibody dilution and incubation time can be optimized. In addition, the incubation time with tyramide reagent for step 3.1.17 can be shortened and the working concentration of tyramide

reagent can be decreased. If there is high background, primary antibody dilution and incubation time can be optimized. Also, the concentration of secondary antibody can be decreased and incubation time with tyramide reagent for step 3.1.17 can be shortened. Include a primary antibody only and a second antibody only staining control can help on which action is needed to optimize the staining condition. Here, staining of a transfected protein (Flag-TRPM7-KR) is carried out with staining controls to optimize the condition. This protein is normally weakly stained with standard immunostaining procedure using Alexa Fluor™ 594 secondary antibody.
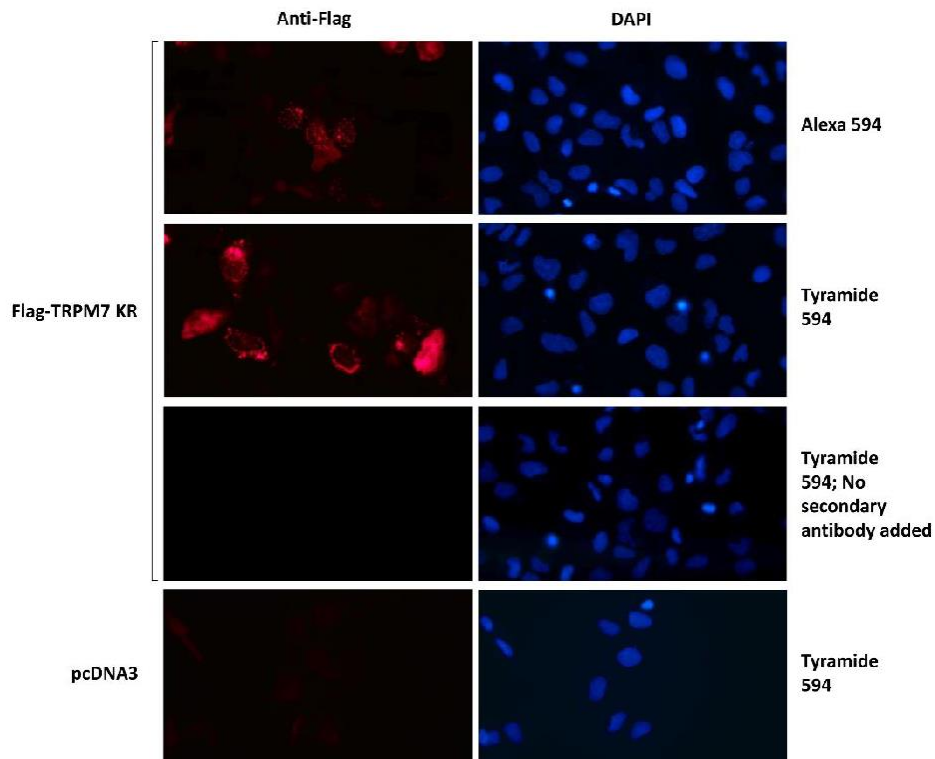

Figure III. 3. Optimizing staining condition for tyramide signal amplification using a transfected protein. U2OS cells were transfected with Flag-TRPM7-KR or empty vector pcDNA3 and then subjected to immunostaining using anti-Flag antibody with goat anti-rabbit IgG (H+L) Alexa Fluor™ 594 secondary antibody or Alexa Fluor™ 594 Tyramide SuperBoost™ Kit, goat anti-rabbit IgG.

Chapter IV. Future Direction

Despite our data shown in Chapter II indicates MDMX is degraded by 20S proteasome ina ubiquitin-independent manner upon zinc-depletion treatment, more experiments need to be carried out to determine the detail mechanism. First, it would be intriguing to know how MDMX is delivered to 20S proteasome. In order to be degraded by proteolytic enzymes locating in inner rings of 20S proteasome, substrates have to be recognized by alpha subunitson outer rings. Although MDM2 has been shown to direct p21 and Rb to 20S proteasome independent of ubiquitination through its interaction with 20S subunit alpha 7, it may not beinvolved in 20S proteasome-mediated MDMX degradation. We have showed that MDM2 depletion by siRNA or MDM2 PROTAC degrader doesn't rescue TPEN-induced MDMX reduction. To support our conclusion, we will further examine the involvement of MDM2 usingMEF cells with or without *mdm2* deletion. In addition, we will explore the hypothesis that MDMX directly interacts with 20S proteasome. Since MDM2 and MDMX share high homologue and it has been shown that the Ring domain of MDM2 is required for 20S subunit-substrate interaction, it is possible that MDMX can also directly interact with 20S proteasomesubunits. Immunoprecipitation of different 20S proteasome subunits and MDMX will be carried out to test the hypothesis. Alternatively, an unknown protein(s) facilitates the interaction between MDMX and 20S proteasome. Proteomic analysis of MDMX binding proteins in the presence of TPEN and MG132 may give answers for that.

We have observed that TRPM7 overexpression leads to a migration change of MDMX onSDS-PAGE. It will be interesting to know if this is due to the post-translational modifications of MDMX and how TRPM7 is involved. As a bi-functional enzyme, cleaved c-terminal domain of TRPM7 has been shown to phosphorylate several proteins including histones. It will be worthto test if TRPM7 can target MDMX for phosphorylation. In addition, it has been shown that TRPM7 often forms heterodimer with TRPM6 for its function. We will further examine if TRPM6 also participates in regulating MDMX stability.

References

1. Abiria, S. A., Krapivinsky, G., Sah, R., Santa-Cruz, A. G., Chaudhuri, D., Zhang, J., . . . Clapham, D. E. (2017). TRPM7 senses oxidative stress to release Zn(2+) from unique intracellular vesicles. *Proc Natl Acad Sci U S A, 114*(30), E6079-E6088. doi:10.1073/pnas.1707380114

2. Abiria, S. A., Krapivinsky, G., Sah, R., Santa-Cruz, A. G., Chaudhuri, D., Zhang, J., . . . Clapham, D. E. (2017). TRPM7 senses oxidative stress to release Zn2+ from unique intracellular vesicles. *Proceedings of the National Academy of Sciences, 114*(30), E6079-E6088. doi:10.1073/pnas.1707380114

3. Alinejad, V., Dolati, S., Motallebnezhad, M., & Yousefi, M. (2017). The role of IL17B-IL17RB signaling pathway in breast cancer. *Biomed Pharmacother, 88*, 795-803. doi:10.1016/j.biopha.2017.01.120

4. Asher, G., Tsvetkov, P., Kahana, C., & Shaul, Y. (2005). A mechanism of ubiquitin-independent proteasomal degradation of the tumor suppressors p53 and p73. *Genes Dev, 19*(3), 316-321. doi:10.1101/gad.319905

5. Ben-Nissan, G., & Sharon, M. (2014). Regulating the 20S proteasome ubiquitin-independent degradation pathway. *Biomolecules, 4*(3), 862-884. doi:10.3390/biom4030862

6. Bie, Q., Zhang, B., Sun, C., Ji, X., Barnie, P. A., Qi, C., . . . Xu, H. (2017). IL-17B activated mesenchymal stem cells enhance proliferation and migration of gastric cancer cells. *Oncotarget, 8*(12), 18914-18923. doi:10.18632/oncotarget.14835

7. Blickwedehl, J., Agarwal, M., Seong, C., Pandita, R. K., Melendy, T., Sung, P., . . . Bangia, N. (2008). Role for proteasome activator PA200 and postglutamyl proteasome activity in genomic stability. *Proc Natl Acad Sci U S A, 105*(42), 16165-16170. doi:10.1073/pnas.0803145105

8. Böttger, A., Böttger, V., Garcia-Echeverria, C., Chène, P., Hochkeppel, H.-K., Sampson, W., . . . Lane, D. P. (1997). Molecular characterization of the hdm2-p53 interaction11Edited by J. Karn. *Journal of Molecular Biology, 269*(5), 744-756. doi:https://doi.org/10.1006/jmbi.1997.1078

9. Candau, R., Scolnick, D. M., Darpino, P., Ying, C. Y., Halazonetis, T. D., & Berger, S. L. (1997). Two tandem and independent sub-activation domains in the amino terminus of p53 require the adaptor complex for activity. *Oncogene, 15*(7), 807-816. doi:10.1038/sj.onc.1201244

10. Cascio, P., Call, M., Petre, B. M., Walz, T., & Goldberg, A. L. (2002). Properties of the hybrid form of the 26S proteasome containing both 19S and PA28 complexes. *Embo j, 21*(11), 2636-2645. doi:10.1093/emboj/21.11.2636

11. Chan, T. A., Hermeking, H., Lengauer, C., Kinzler, K. W., & Vogelstein, B. (1999). 14-3-3σ is required to prevent mitotic catastrophe after DNA damage. *Nature, 401*(6753), 616-620. doi:10.1038/44188

12. Chang, J., Kim, D. H., Lee, S. W., Choi, K. Y., & Sung, Y. C. (1995). Transactivation ability of p53 transcriptional activation domain is directly related to the binding affinity to TATA-binding protein. *J Biol Chem, 270*(42), 25014-25019. doi:10.1074/jbc.270.42.25014

13. Chen, J., Marechal, V., & Levine, A. J. (1993). Mapping of the p53 and mdm-2 interaction domains. *Mol Cell Biol, 13*(7), 4107-4114. doi:10.1128/mcb.13.7.4107

14. Chen, L., Gilkes, D. M., Pan, Y., Lane, W. S., & Chen, J. (2005). ATM and Chk2-dependent

phosphorylationof MDMX contribute to p53 activation after DNA damage. *The EMBO Journal, 24*(19), 3411-3422. doi:https://doi.org/10.1038/sj.emboj.7600812

15. Chen, L., Li, C., Pan, Y., & Chen, J. (2005). Regulation of p53-MDMX interaction by casein kinase 1 alpha.
Molecular and Cellular Biology, 25(15), 6509-6520. doi:10.1128/MCB.25.15.6509-6520.2005

16. Cho, Y., Gorina, S., Jeffrey, P. D., & Pavletich, N. P. (1994). Crystal structure of a p53 tumor suppressor-DNAcomplex: understanding tumorigenic mutations. *Science, 265*(5170), 346-355. doi:10.1126/science.8023157

17. Cho, Y. E., Lomeda, R. A., Ryu, S. H., Lee, J. H., Beattie, J. H., & Kwun, I. S. (2007). Cellular Zn depletion bymetal ion chelators (TPEN, DTPA and chelex resin) and its application to osteoblastic MC3T3-E1 cells. *Nutr Res Pract, 1*(1), 29-35. doi:10.4162/nrp.2007.1.1.29

18. Chubanov, V., Schafer, S., Ferioli, S., & Gudermann, T. (2014). Natural and Synthetic Modulators of the TRPM7 Channel. *Cells, 3*(4), 1089-1101. doi:10.3390/cells3041089

19. Clark, K., Middelbeek, J., Lasonder, E., Dulyaninova, N. G., Morrice, N. A., Ryazanov, A. G., . . . van Leeuwen,
F. N. (2008). TRPM7 regulates myosin IIA filament stability and protein localization by heavy chain phosphorylation. *J Mol Biol, 378*(4), 790-803. doi:10.1016/j.jmb.2008.02.057

20. Cong, L., Ran, F. A., Cox, D., Lin, S., Barretto, R., Habib, N., . . . Zhang, F. (2013). Multiplex genome engineering using CRISPR/Cas systems. *Science, 339*(6121), 819-823. doi:10.1126/science.1231143

21. Dai, M. S., & Lu, H. (2004). Inhibition of MDM2-mediated p53 ubiquitination and degradation by ribosomal protein L5. *J Biol Chem, 279*(43), 44475-44482. doi:10.1074/jbc.M403722200

22. de Polo, A., Vivekanandan, V., Little, J. B., & Yuan, Z. M. (2016). MDMX under stress: the MDMX-MDM2 complex as stress signals hub. *Transl Cancer Res, 5*(6), 725-732. doi:10.21037/tcr.2016.12.18

23. Demeuse, P., Penner, R., & Fleig, A. (2006). TRPM7 channel is regulated by magnesium nucleotides via itskinase domain. *J Gen Physiol, 127*(4), 421-434. doi:10.1085/jgp.200509410

24. Desai, B. N., Krapivinsky, G., Navarro, B., Krapivinsky, L., Carter, B. C., Febvay, S., . . . Clapham, D. E. (2012). Cleavage of TRPM7 releases the kinase domain from the ion channel and regulates its participation in Fas- induced apoptosis. *Dev Cell, 22*(6), 1149-1162. doi:10.1016/j.devcel.2012.04.006

25. Dorovkov, M. V., & Ryazanov, A. G. (2004). Phosphorylation of annexin I by TRPM7 channel-kinase. *J Biol Chem, 279*(49), 50643-50646. doi:10.1074/jbc.C400441200

26. Dulić, V., Stein, G. H., Far, D. F., & Reed, S. I. (1998). Nuclear accumulation of p21Cip1 at the onset of mitosis: a role at the G2/M-phase transition. *Mol Cell Biol, 18*(1), 546-557. doi:10.1128/mcb.18.1.546

27. Fahraeus, R., & Olivares-Illana, V. (2014). MDM2's social network. *Oncogene, 33*(35), 4365-4376. doi:10.1038/onc.2013.410

28. Fakharzadeh, S. S., Trusko, S. P., & George, D. L. (1991). Tumorigenic potential associated with enhanced expression of a gene that is amplified in a mouse tumor cell line. *Embo j, 10*(6), 1565-1569.

29. Fang, S., Jensen, J. P., Ludwig, R. L., Vousden, K. H., & Weissman, A. M. (2000). Mdm2 is a RING

finger- dependent ubiquitin protein ligase for itself and p53. *J Biol Chem, 275*(12), 8945-8951. doi:10.1074/jbc.275.12.8945

30. Frank, A. K., Pietsch, E. C., Dumont, P., Tao, J., & Murphy, M. E. (2011). Wild-type and mutant p53 proteins interact with mitochondrial caspase-3. *Cancer Biol Ther, 11*(8), 740-745. doi:10.4161/cbt.11.8.14906

31. Franklin, R. B., & Costello, L. C. (2007). Zinc as an anti-tumor agent in prostate cancer and in other cancers.
Arch Biochem Biophys, 463(2), 211-217. doi:10.1016/j.abb.2007.02.033

32. Freedman, D. A., Epstein, C. B., Roth, J. C., & Levine, A. J. (1997). A genetic approach to mapping the p53binding site in the MDM2 protein. *Mol Med, 3*(4), 248-259.

33. Gentiletti, F., Mancini, F., D'Angelo, M., Sacchi, A., Pontecorvi, A., Jochemsen, A. G., & Moretti, F. (2002). MDMX stability is regulated by p53-induced caspase cleavage in NIH3T3 mouse fibroblasts. *Oncogene, 21*(6), 867-877. doi:10.1038/sj.onc.1205137

34. Gilkes, D. M., Chen, L., & Chen, J. (2006). MDMX regulation of p53 response to ribosomal stress. *The EMBOJournal, 25*(23), 5614-5625. doi:10.1038/sj.emboj.7601424

35. Giulivi, C., Pacifici, R. E., & Davies, K. J. (1994). Exposure of hydrophobic moieties promotes the selective degradation of hydrogen peroxide-modified hemoglobin by the multicatalytic proteinase complex, proteasome. *Arch Biochem Biophys, 311*(2), 329-341. doi:10.1006/abbi.1994.1245

36. Goldberg, Z., Vogt Sionov, R., Berger, M., Zwang, Y., Perets, R., Van Etten, R. A., . . . Haupt, Y. (2002). Tyrosine phosphorylation of Mdm2 by c-Abl: implications for p53 regulation. *Embo j, 21*(14), 3715-3727. doi:10.1093/emboj/cdf384

37. Grattan, B. J., & Freake, H. C. (2012). Zinc and cancer: implications for LIV-1 in breast cancer. *Nutrients, 4*(7),648-675. doi:10.3390/nu4070648

38. Groll, M., Heinemeyer, W., Jäger, S., Ullrich, T., Bochtler, M., Wolf, D. H., & Huber, R. (1999). The catalytic sites of 20S proteasomes and their role in subunit maturation: a mutational and crystallographic study. *Proc Natl Acad Sci U S A, 96*(20), 10976-10983. doi:10.1073/pnas.96.20.10976

39. Grossman, S. R., Deato, M. E., Brignone, C., Chan, H. M., Kung, A. L., Tagami, H., . . . Livingston, D. M. (2003). Polyubiquitination of p53 by a ubiquitin ligase activity of p300. *Science, 300*(5617), 342-344. doi:10.1126/science.1080386

40. Grossman, S. R., Perez, M., Kung, A. L., Joseph, M., Mansur, C., Xiao, Z. X., . . . Livingston, D. M. (1998). p300/MDM2 complexes participate in MDM2-mediated p53 degradation. *Mol Cell, 2*(4), 405-415. doi:10.1016/s1097-2765(00)80140-9

41. Gu, W., & Roeder, R. G. (1997). Activation of p53 sequence-specific DNA binding by acetylation of the p53 C-terminal domain. *Cell, 90*(4), 595-606. doi:10.1016/s0092-8674(00)80521-8

42. Guilbert, A., Gautier, M., Dhennin-Duthille, I., Haren, N., Sevestre, H., & Ouadid-Ahidouch, H. (2009). Evidence that TRPM7 is required for breast cancer cell proliferation. *Am J Physiol Cell Physiol, 297*(3), C493-502. doi:10.1152/ajpcell.00624.2008

43. Harper, J. W., Adami, G. R., Wei, N., Keyomarsi, K., & Elledge, S. J. (1993). The p21 Cdk-interacting proteinCip1 is a potent inhibitor of G1 cyclin-dependent kinases. *Cell, 75*(4), 805-816. doi:10.1016/0092- 8674(93)90499-g

44. Hashemi, M., Ghavami, S., Eshraghi, M., Booy, E. P., & Los, M. (2007). Cytotoxic effects of intra and extracellular zinc chelation on human breast cancer cells. *Eur J Pharmacol, 557*(1), 9-19. doi:10.1016/j.ejphar.2006.11.010

45. Haupt, Y., Maya, R., Kazaz, A., & Oren, M. (1997). Mdm2 promotes the rapid degradation of p53. *Nature, 387*(6630), 296-299. doi:10.1038/387296a0

46. Hermeking, H., Lengauer, C., Polyak, K., He, T.-C., Zhang, L., Thiagalingam, S., . . . Vogelstein, B. (1997). 14-3-3σ Is a p53-Regulated Inhibitor of G2/M Progression. *Molecular Cell, 1*(1), 3-11. doi:https://doi.org/10.1016/S1097-2765(00)80002-7

47. Hershko, A., & Ciechanover, A. (1998). The ubiquitin system. *Annu Rev Biochem, 67*, 425-479. doi:10.1146/annurev.biochem.67.1.425

48. Ho, E., Courtemanche, C., & Ames, B. N. (2003). Zinc deficiency induces oxidative DNA damage and increases p53 expression in human lung fibroblasts. *J Nutr, 133*(8), 2543-2548. doi:10.1093/jn/133.8.2543

49. Hollstein, M., Sidransky, D., Vogelstein, B., & Harris, C. C. (1991). p53 mutations in human cancers. *Science,253*(5015), 49-53.

50. Huang, L., Yan, Z., Liao, X., Li, Y., Yang, J., Wang, Z.-G., . . . Yuan, Z.-M. (2011). The p53 inhibitors MDM2/MDMX complex is required for control of p53 activity in vivo. *Proceedings of the National Academy ofSciences, 108*(29), 12001. doi:10.1073/pnas.1102309108

51. Hunyady, B., Krempels, K., Harta, G., & Mezey, E. (1996). Immunohistochemical signal amplification by catalyzed reporter deposition and its application in double immunostaining. *J Histochem Cytochem, 44*(12), 1353-1362.

52. Inoue, K., O'Bryant, Z., & Xiong, Z. G. (2015). Zinc-permeable ion channels: effects on intracellular zinc dynamics and potential physiological/pathophysiological significance. *Curr Med Chem, 22*(10), 1248-1257.

    doi:10.2174/0929867322666150209153750

53. Ito, A., Kawaguchi, Y., Lai, C. H., Kovacs, J. J., Higashimoto, Y., Appella, E., & Yao, T. P. (2002). MDM2- HDAC1-mediated deacetylation of p53 is required for its degradation. *Embo j, 21*(22), 6236-6245. doi:10.1093/emboj/cdf616

54. Jackson, M. W., & Berberich, S. J. (1999). Constitutive mdmx expression during cell growth, differentiation, and DNA damage. *DNA Cell Biol, 18*(9), 693-700. doi:10.1089/104454999314971

55. Jackson, M. W., Lindstrom, M. S., & Berberich, S. J. (2001). MdmX binding to ARF affects Mdm2 protein stability and p53 transactivation. *J Biol Chem, 276*(27), 25336-25341. doi:10.1074/jbc.M010685200

56. Jin, J., Desai, B. N., Navarro, B., Donovan, A., Andrews, N. C., & Clapham, D. E. (2008). Deletion of Trpm7 disrupts embryonic development and thymopoiesis without altering Mg2+ homeostasis. *Science, 322*(5902),756-760. doi:10.1126/science.1163493

57. Jin, J., Wu, L. J., Jun, J., Cheng, X., Xu, H., Andrews, N. C., & Clapham, D. E. (2012). The channel kinase, TRPM7, is required for early embryonic development. *Proc Natl Acad Sci U S A, 109*(5), E225-233. doi:10.1073/pnas.1120033109

58. Jin, Y., Dai, M.-S., Lu, S. Z., Xu, Y., Luo, Z., Zhao, Y., & Lu, H. (2006). 14-3-3gamma binds to MDMX that is phosphorylated by UV-activated Chk1, resulting in p53 activation. *The EMBO*

Journal, 25(6), 1207-1218. doi:10.1038/sj.emboj.7601010

59. Jin, Y., Lee, H., Zeng, S. X., Dai, M. S., & Lu, H. (2003). MDM2 promotes p21waf1/cip1 proteasomal turnoverindependently of ubiquitylation. *EMBO J, 22*(23), 6365-6377. doi:10.1093/emboj/cdg600

60. Kambe, T., Tsuji, T., Hashimoto, A., & Itsumura, N. (2015). The Physiological, Biochemical, and Molecular Roles of Zinc Transporters in Zinc Homeostasis and Metabolism. *Physiol Rev, 95*(3), 749-784. doi:10.1152/physrev.00035.2014

61. Kawaguchi, T., Kato, S., Otsuka, K., Watanabe, G., Kumabe, T., Tominaga, T., . . . Ishioka, C. (2005). The relationship among p53 oligomer formation, structure and transcriptional activity using a comprehensive missense mutation library. *Oncogene, 24*(46), 6976-6981. doi:10.1038/sj.onc.1208839

62. Kawai, H., Lopez-Pajares, V., Kim, M. M., Wiederschain, D., & Yuan, Z. M. (2007). RING domain-mediated interaction is a requirement for MDM2's E3 ligase activity. *Cancer Res, 67*(13), 6026-6030. doi:10.1158/0008-5472.CAN-07-1313

63. Kawai, H., Wiederschain, D., Kitao, H., Stuart, J., Tsai, K. K., & Yuan, Z. M. (2003). DNA damage-induced MDMX degradation is mediated by MDM2. *J Biol Chem, 278*(46), 45946-45953. doi:10.1074/jbc.M308295200

64. Khosravi, R., Maya, R., Gottlieb, T., Oren, M., Shiloh, Y., & Shkedy, D. (1999). Rapid ATM-dependent phosphorylation of MDM2 precedes p53 accumulation in response to DNA damage. *Proc Natl Acad Sci U S A, 96*(26), 14973-14977. doi:10.1073/pnas.96.26.14973

65. Kisselev, A. F., Kaganovich, D., & Goldberg, A. L. (2002). Binding of hydrophobic peptides to several non- catalytic sites promotes peptide hydrolysis by all active sites of 20 S proteasomes. Evidence for peptide- induced channel opening in the alpha-rings. *J Biol Chem, 277*(25), 22260-22270. doi:10.1074/jbc.M112360200

66. Kitagaki, J., Agama, K. K., Pommier, Y., Yang, Y., & Weissman, A. M. (2008). Targeting tumor cells expressing p53 with a water-soluble inhibitor of Hdm2. *Mol Cancer Ther, 7*(8), 2445-2454. doi:10.1158/1535-7163.MCT-08-0063

67. Kobet, E., Zeng, X., Zhu, Y., Keller, D., & Lu, H. (2000). MDM2 inhibits p300-mediated p53 acetylation and activation by forming a ternary complex with the two proteins. *Proceedings of the National Academy of Sciences, 97*(23), 12547. doi:10.1073/pnas.97.23.12547

68. Koegl, M., Hoppe, T., Schlenker, S., Ulrich, H. D., Mayer, T. U., & Jentsch, S. (1999). A novel ubiquitination
factor, E4, is involved in multiubiquitin chain assembly. *Cell, 96*(5), 635-644. doi:10.1016/s0092-8674(00)80574-7

69. Kolls, J. K., & Linden, A. (2004). Interleukin-17 family members and inflammation. *Immunity, 21*(4), 467-476.doi:10.1016/j.immuni.2004.08.018

70. Komander, D. (2009). The emerging complexity of protein ubiquitination. *Biochem Soc Trans, 37*(Pt 5), 937-953. doi:10.1042/bst0370937

71. Krapivinsky, G., Krapivinsky, L., Manasian, Y., & Clapham, D. E. (2014). The TRPM7 chanzyme is cleaved to release a chromatin-modifying kinase. *Cell, 157*(5), 1061-1072. doi:10.1016/j.cell.2014.03.046

72. Kubbutat, M. H. G., Jones, S. N., & Vousden, K. H. (1997). Regulation of p53 stability by Mdm2. *Nature, 387*(6630), 299-303. doi:10.1038/387299a0

73. Kulikov, R., Letienne, J., Kaur, M., Grossman, S. R., Arts, J., & Blattner, C. (2010). Mdm2 facilitates the association of p53 with the proteasome. *Proc Natl Acad Sci U S A, 107*(22), 10038-10043. doi:10.1073/pnas.0911716107

74. Kussie, P. H., Gorina, S., Marechal, V., Elenbaas, B., Moreau, J., Levine, A. J., & Pavletich, N. P. (1996). Structure of the MDM2 oncoprotein bound to the p53 tumor suppressor transactivation domain. *Science, 274*(5289), 948-953. doi:10.1126/science.274.5289.948

75. Lai, Z., Freedman, D. A., Levine, A. J., & McLendon, G. L. (1998). Metal and RNA binding properties of the hdm2 RING finger domain. *Biochemistry, 37*(48), 7005-7015. doi:10.1021/bi980596r

76. LeBron, C., Chen, L., Gilkes, D. M., & Chen, J. (2006). Regulation of MDMX nuclear import and degradation by Chk2 and 14-3-3. *The EMBO Journal, 25*(6), 1196-1206. doi:https://doi.org/10.1038/sj.emboj.7601032

77. Lee, J.-H., Jin, Y., He, G., Zeng, S. X., Wang, Y. V., Wahl, G. M., & Lu, H. (2012). Hypoxia activates tumor suppressor p53 by inducing ATR-Chk1 kinase cascade-mediated phosphorylation and consequent 14-3-3γ inactivation of MDMX protein. *J Biol Chem, 287*(25), 20898-20903. doi:10.1074/jbc.M111.336875

78. Leng, P., Brown, D. R., Shivakumar, C. V., Deb, S., & Deb, S. P. (1995). N-terminal 130 amino acids of MDM2are sufficient to inhibit p53-mediated transcriptional activation. *Oncogene, 10*(7), 1275-1282.

79. Li, M., Brooks, C. L., Wu-Baer, F., Chen, D., Baer, R., & Gu, W. (2003). Mono- versus polyubiquitination: differential control of p53 fate by Mdm2. *Science, 302*(5652), 1972-1975. doi:10.1126/science.1091362

80. Li, M., Du, J., Jiang, J., Ratzan, W., Su, L. T., Runnels, L. W., & Yue, L. (2007). Molecular determinants of Mg2+ and Ca2+ permeability and pH sensitivity in TRPM6 and TRPM7. *J Biol Chem, 282*(35), 25817-25830.doi:10.1074/jbc.M608972200

81. Li, M., & Gu, W. (2011). A critical role for noncoding 5S rRNA in regulating Mdmx stability. *Mol Cell, 43*(6), 1023-1032. doi:10.1016/j.molcel.2011.08.020

82. Li, Y., Yang, J., Aguilar, A., McEachern, D., Przybranowski, S., Liu, L., . . . Wang, S. (2019). Discovery of MD-224 as a First-in-Class, Highly Potent, and Efficacious Proteolysis Targeting Chimera Murine Double Minute2 Degrader Capable of Achieving Complete and Durable Tumor Regression. *J Med Chem, 62*(2), 448-466. doi:10.1021/acs.jmedchem.8b00909

83. Liang, S.-H., & Clarke, M. F. (1999). The nuclear import of p53 is determined by the presence of a basic domain and its relative position to the nuclear localization signal. *Oncogene, 18*(12), 2163-2166. doi:10.1038/sj.onc.1202350

84. Liang, S. H., Hong, D., & Clarke, M. F. (1998). Cooperation of a single lysine mutation and a C-terminal domain in the cytoplasmic sequestration of the p53 protein. *J Biol Chem, 273*(31), 19817-19821. doi:10.1074/jbc.273.31.19817

85. Linares, L. K., Hengstermann, A., Ciechanover, A., Müller, S., & Scheffner, M. (2003). HdmX stimulates Hdm2- mediated ubiquitination and degradation of p53. *Proceedings of the National Academy of Sciences, 100*(21), 12009. doi:10.1073/pnas.2030930100

86. Lindstrom, M. S., Jin, A., Deisenroth, C., White Wolf, G., & Zhang, Y. (2007). Cancer-associated

mutations in the MDM2 zinc finger domain disrupt ribosomal protein interaction and attenuate MDM2-induced p53 degradation. *Mol Cell Biol, 27*(3), 1056-1068. doi:10.1128/MCB.01307-06

87. Lindström, M. S., Jin, A., Deisenroth, C., White Wolf, G., & Zhang, Y. (2007). Cancer-associated mutations in the MDM2 zinc finger domain disrupt ribosomal protein interaction and attenuate MDM2-induced p53 degradation. *Mol Cell Biol, 27*(3), 1056-1068. doi:10.1128/MCB.01307-06

88. Maki, C. G., & Howley, P. M. (1997). Ubiquitination of p53 and p21 is differentially affected by ionizing and UV radiation. *Molecular and Cellular Biology, 17*(1), 355-363. doi:10.1128/mcb.17.1.355

89. Maki, C. G., Huibregtse, J. M., & Howley, P. M. (1996). In vivo ubiquitination and proteasome-mediated degradation of p53(1). *Cancer Res, 56*(11), 2649-2654.

90. Maltzman, W., & Czyzyk, L. (1984). UV irradiation stimulates levels of p53 cellular tumor antigen in nontransformed mouse cells. *Molecular and Cellular Biology, 4*(9), 1689-1694. doi:10.1128/mcb.4.9.1689

91. Mancini, F., Di Conza, G., Pellegrino, M., Rinaldo, C., Prodosmo, A., Giglio, S., . . . Moretti, F. (2009). MDM4 (MDMX) localizes at the mitochondria and facilitates the p53-mediated intrinsic-apoptotic pathway. *Embo j, 28*(13), 1926-1939. doi:10.1038/emboj.2009.154

92. Manfredi, J. J. (2010). The Mdm2-p53 relationship evolves: Mdm2 swings both ways as an oncogene and a tumor suppressor. *Genes Dev, 24*(15), 1580-1589. doi:10.1101/gad.1941710

93. Marine, J. C., & Lozano, G. (2010). Mdm2-mediated ubiquitylation: p53 and beyond. *Cell Death Differ, 17*(1), 93-102. doi:10.1038/cdd.2009.68

94. Matijasevic, Z., Krzywicka-Racka, A., Sluder, G., Gallant, J., & Jones, S. N. (2016). The Zn-finger domain of MdmX suppresses cancer progression by promoting genome stability in p53-mutant cells. *Oncogenesis, 5*(10), e262. doi:10.1038/oncsis.2016.62

95. Maya, R., Balass, M., Kim, S. T., Shkedy, D., Leal, J. F., Shifman, O., . . . Oren, M. (2001). ATM-dependent phosphorylation of Mdm2 on serine 395: role in p53 activation by DNA damage. *Genes Dev, 15*(9), 1067- 1077. doi:10.1101/gad.886901

96. Meek, D. W. (2015). Regulation of the p53 response and its relationship to cancer. *Biochem J, 469*(3), 325- 346. doi:10.1042/BJ20150517

97. Meulmeester, E., Maurice, M. M., Boutell, C., Teunisse, A. F. A. S., Ovaa, H., Abraham, T. E., . . . Jochemsen,
A. G. (2005). Loss of HAUSP-Mediated Deubiquitination Contributes to DNA Damage-Induced Destabilization of Hdmx and Hdm2. *Molecular Cell, 18*(5), 565-576. doi:https://doi.org/10.1016/j.molcel.2005.04.024

98. Middelbeek, J., Kuipers, A. J., Henneman, L., Visser, D., Eidhof, I., van Horssen, R., . . . Jalink, K. (2012). TRPM7 is required for breast tumor cell metastasis. *Cancer Res, 72*(16), 4250-4261. doi:10.1158/0008- 5472.CAN-11-3863

99. Mihara, M., Erster, S., Zaika, A., Petrenko, O., Chittenden, T., Pancoska, P., & Moll, U. M. (2003). p53 Has a Direct Apoptogenic Role at the Mitochondria. *Molecular Cell, 11*(3), 577-590. doi:https://doi.org/10.1016/S1097-2765(03)00050-9

100. Milner, J., & Medcalf, E. A. (1991). Cotranslation of activated mutant p53 with wild type drives the wild-type p53 protein into the mutant conformation. *Cell, 65*(5), 765-774. doi:10.1016/0092-8674(91)90384-b

101. Mocchegiani, E., Muzzioli, M., & Giacconi, R. (2000). Zinc and immunoresistance to infection in aging: new biological tools. *Trends Pharmacol Sci, 21*(6), 205-208.

102. Momand, J., Jung, D., Wilczynski, S., & Niland, J. (1998). The MDM2 gene amplification database. *Nucleic Acids Res, 26*(15), 3453-3459. doi:10.1093/nar/26.15.3453

103. Monin, L., & Gaffen, S. L. (2018). Interleukin 17 Family Cytokines: Signaling Mechanisms, Biological Activities, and Therapeutic Implications. *Cold Spring Harb Perspect Biol, 10*(4). doi:10.1101/cshperspect.a028522

104. Monteilh-Zoller, M. K., Hermosura, M. C., Nadler, M. J., Scharenberg, A. M., Penner, R., & Fleig, A. (2003). TRPM7 provides an ion channel mechanism for cellular entry of trace metal ions. *J Gen Physiol, 121*(1), 49-60. doi:10.1085/jgp.20028740

105. Oda, K., Arakawa, H., Tanaka, T., Matsuda, K., Tanikawa, C., Mori, T., . . . Taya, Y. (2000). p53AIP1, a potential mediator of p53-dependent apoptosis, and its regulation by Ser-46-phosphorylated p53. *Cell, 102*(6), 849- 862. doi:10.1016/s0092-8674(00)00073-8

106. Okamoto, K., Kashima, K., Pereg, Y., Ishida, M., Yamazaki, S., Nota, A., . . . Taya, Y. (2005). DNA Damage-Induced Phosphorylation of MdmX at Serine 367 Activates p53 by Targeting MdmX for Mdm2-Dependent Degradation. *Molecular and Cellular Biology, 25*(21), 9608. doi:10.1128/MCB.25.21.9608-9620.2005

107. Oliner, J. D., Kinzler, K. W., Meltzer, P. S., George, D. L., & Vogelstein, B. (1992). Amplification of a gene encoding a p53-associated protein in human sarcomas. *Nature, 358*(6381), 80-83. doi:10.1038/358080a0

108. Ortega, J., Heymann, J. B., Kajava, A. V., Ustrell, V., Rechsteiner, M., & Steven, A. C. (2005). The axial channel of the 20S proteasome opens upon binding of the PA200 activator. *J Mol Biol, 346*(5), 1221-1227. doi:10.1016/j.jmb.2004.12.049

109. Pan, Z., Choi, S., Ouadid-Ahidouch, H., Yang, J. M., Beattie, J. H., & Korichneva, I. (2017). Zinc transporters and dysregulated channels in cancers. *Front Biosci (Landmark Ed), 22*, 623-643. doi:10.2741/4507

110. Parant, J., Chavez-Reyes, A., Little, N. A., Yan, W., Reinke, V., Jochemsen, A. G., & Lozano, G. (2001). Rescue of embryonic lethality in Mdm4-null mice by loss of Trp53 suggests a nonoverlapping pathway with MDM2 to regulate p53. *Nat Genet, 29*(1), 92-95. doi:10.1038/ng714

111. Parra, E. R., Uraoka, N., Jiang, M., Cook, P., Gibbons, D., Forget, M. A., . . . Rodriguez-Canales, J. (2017). Validation of multiplex immunofluorescence panels using multispectral microscopy for immune-profiling of formalin-fixed and paraffin-embedded human tumor tissues. *Sci Rep, 7*(1), 13380. doi:10.1038/s41598-017- 13942-8

112. Pereg, Y., Lam, S., Teunisse, A., Biton, S., Meulmeester, E., Mittelman, L., . . . Jochemsen, A. G. (2006). Differential Roles of ATM- and Chk2-Mediated Phosphorylations of Hdmx in Response to DNA Damage. *Molecular and Cellular Biology, 26*(18), 6819. doi:10.1128/MCB.00562-06

113. Pereg, Y., Shkedy, D., de Graaf, P., Meulmeester, E., Edelson-Averbukh, M., Salek, M., . . . Shiloh, Y. (2005). Phosphorylation of Hdmx mediates its Hdm2- and ATM-dependent degradation in response to DNA damage. *Proc Natl Acad Sci U S A, 102*(14), 5056-5061. doi:10.1073/pnas.0408595102

114. Pickart, C. M. (2001). Mechanisms underlying ubiquitination. *Annu Rev Biochem, 70*, 503-533. doi:10.1146/annurev.biochem.70.1.503

115. Pickering, A. M., & Davies, K. J. (2012). Differential roles of proteasome and immunoproteasome regulators Pa28αβ, Pa28γ and Pa200 in the degradation of oxidized proteins. *Arch Biochem Biophys, 523*(2), 181-190.doi:10.1016/j.abb.2012.04.018

116. Pietsch, E. C., Perchiniak, E., Canutescu, A. A., Wang, G., Dunbrack, R. L., & Murphy, M. E. (2008). Oligomerization of BAK by p53 utilizes conserved residues of the p53 DNA binding domain. *J Biol Chem, 283*(30), 21294-21304. doi:10.1074/jbc.M710539200

117. Popowicz, G. M., Czarna, A., & Holak, T. A. (2008). Structure of the human Mdmx protein bound to the p53 tumor suppressor transactivation domain. *Cell Cycle, 7*(15), 2441-2443. doi:10.4161/cc.6365

118. Ra, H., Kim, H. L., Lee, H. W., & Kim, Y. H. (2009). Essential role of p53 in TPEN-induced neuronal apoptosis. *FEBS Lett, 583*(9), 1516-1520. doi:10.1016/j.febslet.2009.04.008

119. Ren, L., Xu, Y., Liu, C., Wang, S., & Qin, G. (2017). IL-17RB enhances thyroid cancer cell invasion and metastasis via ERK1/2 pathway-mediated MMP-9 expression. *Mol Immunol, 90*, 126-135. doi:10.1016/j.molimm.2017.06.034

120. Ruaro, E. M., Collavin, L., Del Sal, G., Haffner, R., Oren, M., Levine, A. J., & Schneider, C. (1997). A proline- rich motif in p53 is required for transactivation- independent growth arrest as induced by Gas1. *Proceedings of the National Academy of Sciences, 94*, 4675-4680.

121. Runnels, L. W., Yue, L., & Clapham, D. E. (2001). TRP-PLIK, a bifunctional protein with kinase and ion channel activities. *Science, 291*(5506), 1043-1047. doi:10.1126/science.1058519

122. Ryazanova, L. V., Dorovkov, M. V., Ansari, A., & Ryazanov, A. G. (2004). Characterization of the protein kinase activity of TRPM7/ChaK1, a protein kinase fused to the transient receptor potential ion channel. *J Biol Chem, 279*(5), 3708-3716. doi:10.1074/jbc.M308820200

123. Scheffner, M., Nuber, U., & Huibregtse, J. M. (1995). Protein ubiquitination involving an E1-E2-E3 enzyme ubiquitin thioester cascade. *Nature, 373*(6509), 81-83. doi:10.1038/373081a0

124. Schmitz, C., Perraud, A. L., Johnson, C. O., Inabe, K., Smith, M. K., Penner, R., . . . Scharenberg, A. M. (2003). Regulation of vertebrate cellular Mg2+ homeostasis by TRPM7. *Cell, 114*(2), 191-200. doi:10.1016/s0092- 8674(03)00556-7

125. Sdek, P., Ying, H., Chang, D. L., Qiu, W., Zheng, H., Touitou, R., . . . Xiao, Z. X. (2005). MDM2 promotes proteasome-dependent ubiquitin-independent degradation of retinoblastoma protein. *Mol Cell, 20*(5), 699-708. doi:10.1016/j.molcel.2005.10.017

126. Sdek, P., Ying, H., Chang, D. L. F., Qiu, W., Zheng, H., Touitou, R., . . . Jim Xiao, Z.-X. (2005). MDM2 Promotes Proteasome-Dependent Ubiquitin-Independent Degradation of Retinoblastoma Protein. *Mol Cell, 20*(5), 699-708. doi:https://doi.org/10.1016/j.molcel.2005.10.017

127. Sharp, D. A., Kratowicz, S. A., Sank, M. J., & George, D. L. (1999). Stabilization of the MDM2 Oncoprotein by Interaction with the Structurally Related MDMX Protein*. *Journal of Biological Chemistry, 274*(53), 38189- 38196. doi:https://doi.org/10.1074/jbc.274.53.38189

128. Sherr, C. J. (2006). Divorcing ARF and p53: an unsettled case. *Nature Reviews Cancer, 6*(9), 663-673. doi:10.1038/nrc1954

129. Shi, D., & Gu, W. (2012). Dual Roles of MDM2 in the Regulation of p53: Ubiquitination Dependent and Ubiquitination Independent Mechanisms of MDM2 Repression of p53 Activity. *Genes & cancer, 3*(3-4), 240- 248. doi:10.1177/1947601912455199

130. Shi, D., Pop, M. S., Kulikov, R., Love, I. M., Kung, A. L., & Grossman, S. R. (2009). CBP and p300 are cytoplasmic E4 polyubiquitin ligases for p53. *Proc Natl Acad Sci U S A, 106*(38), 16275-16280. doi:10.1073/pnas.0904305106

131. Shvarts, A., Bazuine, M., Dekker, P., Ramos, Y. F., Steegenga, W. T., Merckx, G., . . . Jochemsen, A. G. (1997).Isolation and identification of the human homolog of a new p53-binding protein, Mdmx. *Genomics, 43*(1), 34-42. doi:10.1006/geno.1997.4775

132. Shvarts, A., Steegenga, W. T., Riteco, N., van Laar, T., Dekker, P., Bazuine, M., . . . Jochemsen, A. G. (1996). MDMX: a novel p53-binding protein with some functional properties of MDM2. *Embo j, 15*(19), 5349-5357.

133. Sionov, R. V., Coen, S., Goldberg, Z., Berger, M., Bercovich, B., Ben-Neriah, Y., . . . Haupt, Y. (2001). c-Abl regulates p53 levels under normal and stress conditions by preventing its nuclear export and ubiquitination. *Mol Cell Biol, 21*(17), 5869-5878. doi:10.1128/mcb.21.17.5869-5878.2001

134. Soussi, T., & Beroud, C. (2001). Assessing TP53 status in human tumours to evaluate clinical outcome. *NatRev Cancer, 1*(3), 233-240. doi:10.1038/35106009

135. St Clair, S., Giono, L., Varmeh-Ziaie, S., Resnick-Silverman, L., Liu, W. J., Padi, A., . . . Manfredi, J. J. (2004). DNA damage-induced downregulation of Cdc25C is mediated by p53 via two independent mechanisms: oneinvolves direct binding to the cdc25C promoter. *Mol Cell, 16*(5), 725-736. doi:10.1016/j.molcel.2004.11.002

136. Stack, E. C., Wang, C., Roman, K. A., & Hoyt, C. C. (2014). Multiplexed immunohistochemistry, imaging, and quantitation: a review, with an assessment of Tyramide signal amplification, multispectral imaging and multiplex analysis. *Methods, 70*(1), 46-58. doi:10.1016/j.ymeth.2014.08.016

137. Stommel, J. M., Marchenko, N. D., Jimenez, G. S., Moll, U. M., Hope, T. J., & Wahl, G. M. (1999). A leucine-rich nuclear export signal in the p53 tetramerization domain: regulation of subcellular localization and p53 activity by NES masking. *The EMBO Journal, 18*(6), 1660-1672. doi:https://doi.org/10.1093/emboj/18.6.1660

138. Stoner, C. S., Pearson, G. D., Koc, A., Merwin, J. R., Lopez, N. I., & Merrill, G. F. (2009). Effect of thioredoxin deletion and p53 cysteine replacement on human p53 activity in wild-type and thioredoxin reductase null yeast.*Biochemistry, 48*(38), 9156-9169. doi:10.1021/bi900757q

139. Tanimura, S., Ohtsuka, S., Mitsui, K., Shirouzu, K., Yoshimura, A., & Ohtsubo, M. (1999). MDM2 interacts with MDMX through their RING finger domains. *FEBS Lett, 447*(1), 5-9. doi:10.1016/s0014-5793(99)00254-9

140. Touitou, R., Richardson, J., Bose, S., Nakanishi, M., Rivett, J., & Allday, M. J. (2001). A degradation signal located in the C-terminus of p21WAF1/CIP1 is a binding site for the C8 alpha-subunit of the 20S proteasome.*Embo j, 20*(10), 2367-2375. doi:10.1093/emboj/20.10.2367

141. Vasak, M., & Hasler, D. W. (2000). Metallothioneins: new functional and structural insights. *Curr Opin ChemBiol, 4*(2), 177-183.

142. Venot, C., Maratrat, M., Dureuil, C., Conseiller, E., Bracco, L., & Debussche, L. (1998). The requirement for the p53 proline-rich functional domain for mediation of apoptosis is correlated with specific PIG3 gene transactivation and with transcriptional repression. *The EMBO Journal, 17*(16),

4668-4679. doi:https://doi.org/10.1093/emboj/17.16.4668

143. Vogelstein, B., Lane, D., & Levine, A. J. (2000). Surfing the p53 network. *Nature, 408*(6810), 307-310. doi:10.1038/35042675

144. Vousden, K. H., & Prives, C. (2009). Blinded by the Light: The Growing Complexity of p53. *Cell, 137*(3), 413-431. doi:10.1016/j.cell.2009.04.037

145. Wade, M., Li, Y. C., & Wahl, G. M. (2013). MDM2, MDMX and p53 in oncogenesis and cancer therapy. *Nat Rev Cancer, 13*(2), 83-96. doi:10.1038/nrc3430

146. Wadgaonkar, R., & Collins, T. (1999). Murine double minute (MDM2) blocks p53-coactivator interaction, a new mechanism for inhibition of p53-dependent gene expression. *J Biol Chem, 274*(20), 13760-13767. doi:10.1074/jbc.274.20.13760

147. Wang, B., Liu, K., Lin, H. Y., Bellam, N., Ling, S., & Lin, W. C. (2010). 14-3-3Tau regulates ubiquitin-independent proteasomal degradation of p21, a novel mechanism of p21 downregulation in breast cancer. *Mol Cell Biol, 30*(6), 1508-1527. doi:10.1128/mcb.01335-09

148. Wang, H., Ma, X., Ren, S., Buolamwini, J. K., & Yan, C. (2011). A small-molecule inhibitor of MDMX activatesp53 and induces apoptosis. *Mol Cancer Ther, 10*(1), 69-79. doi:10.1158/1535-7163.MCT-10-0581

149. Warren, R. S., Atreya, C. E., Niedzwiecki, D., Weinberg, V. K., Donner, D. B., Mayer, R. J., . . . Bertagnolli, M.
M. (2013). Association of TP53 mutational status and gender with survival after adjuvant treatment for stage III colon cancer: results of CALGB 89803. *Clin Cancer Res, 19*(20), 5777-5787. doi:10.1158/1078-0432.CCR-13-0351

150. Wei, X., Wu, S., Song, T., Chen, L., Gao, M., Borcherds, W., . . . Chen, J. (2016). Secondary interaction between MDMX and p53 core domain inhibits p53 DNA binding. *Proceedings of the National Academy of Sciences, 113*, E2558-E2563.

151. Wu, H. H., Hwang-Verslues, W. W., Lee, W. H., Huang, C. K., Wei, P. C., Chen, C. L., . . . Lee, W. H. (2015). Targeting IL-17B-IL-17RB signaling with an anti-IL-17RB antibody blocks pancreatic cancer metastasis by silencing multiple chemokines. *J Exp Med, 212*(3), 333-349. doi:10.1084/jem.20141702

152. Xu, J., Patrick, B. A., & Jaiswal, A. K. (2013). NRH:quinone oxidoreductase 2 (NQO2) protein competes with the 20 S proteasome to stabilize transcription factor CCAAT enhancer-binding protein α (C/EBPα), leading toprotection against γ radiation-induced myeloproliferative disease. *J Biol Chem, 288*(48), 34799-34808. doi:10.1074/jbc.M113.495580

153. Yee, N. S. (2017). Role of TRPM7 in Cancer: Potential as Molecular Biomarker and Therapeutic Target.
Pharmaceuticals (Basel), 10(2). doi:10.3390/ph10020039

154. Yee, N. S., Kazi, A. A., & Yee, R. K. (2014). Cellular and Developmental Biology of TRPM7 Channel-Kinase:Implicated Roles in Cancer. *Cells, 3*(3), 751-777. doi:10.3390/cells3030751

155. Yu, S., Qin, D., Shangary, S., Chen, J., Wang, G., Ding, K., . . . Wang, S. (2009). Potent and orally active small-molecule inhibitors of the MDM2-p53 interaction. *J Med Chem, 52*(24), 7970-7973. doi:10.1021/jm901400z

156. Yu, X., Vazquez, A., Levine, A. J., & Carpizo, D. R. (2012). Allele-specific p53 mutant reactivation. *Cancer Cell, 21*(5), 614-625. doi:10.1016/j.ccr.2012.03.042

157. Zhang, Y., Wolf, G. W., Bhat, K., Jin, A., Allio, T., Burkhart, W. A., & Xiong, Y. (2003). Ribosomal protein L11negatively regulates oncoprotein MDM2 and mediates a p53-dependent ribosomal-stress checkpoint pathway. *Mol Cell Biol, 23*(23), 8902-8912. doi:10.1128/mcb.23.23.8902-8912.2003

158. Zhang, Y., Xiong, Y., & Yarbrough, W. G. (1998). ARF promotes MDM2 degradation and stabilizes p53: ARF-INK4a locus deletion impairs both the Rb and p53 tumor suppression pathways. *Cell, 92*(6), 725-734. doi:10.1016/s0092-8674(00)81401-4

159. Zhang, Z., Wang, H., Li, M., Agrawal, S., Chen, X., & Zhang, R. (2004). MDM2 is a negative regulator of p21WAF1/CIP1, independent of p53. *J Biol Chem, 279*(16), 16000-16006. doi:10.1074/jbc.M312264200

160. Zhu, Y., Poyurovsky, M. V., Li, Y., Biderman, L., Stahl, J., Jacq, X., & Prives, C. (2009). Ribosomal protein S7 is both a regulator and a substrate of MDM2. *Mol Cell, 35*(3), 316-326. doi:10.1016/j.molcel.2009.07.014

161. Zuckerman, V., Lenos, K., Popowicz, G. M., Silberman, I., Grossman, T., Marine, J. C., . . . Haupt, Y. (2009).c-Abl phosphorylates Hdmx and regulates its interaction with p53. *J Biol Chem, 284*(6), 4031-4039. doi:10.1074/jbc.M809211200

Vita

Name	*Herui Wang*
Baccalaureate Degree	*Bachelor of Science, Beijing University of Chemical Technology, Beijing* *Major:Biotechnology*
Date Graduated	*07, 2014*